

# Decay properties of the new isotopes $^{188}\text{At}$ and $^{190}\text{At}$

Master's Thesis, 2.5.2023

Author:

HENNA KOKKONEN

Supervisor:

KALLE AURANEN



UNIVERSITY OF JYVÄSKYLÄ  
DEPARTMENT OF PHYSICS

© 2023 Henna Kokkonen

This publication is copyrighted. You may download, display and print it for Your own personal use. Commercial use is prohibited. Julkaisu on tekijänoikeussäännösten alainen. Teosta voi lukea ja tulostaa henkilökohtaista käyttöä varten. Käyttö kaupallisiin tarkoituksiin on kielletty.

## Abstract

Kokkonen, Henna

Decay properties of the new isotopes  $^{188}\text{At}$  and  $^{190}\text{At}$

Master's thesis

Department of Physics, University of Jyväskylä, 2023, 47 pages.

In this thesis new astatine isotopes and their decay properties are studied. The properties of the most neutron deficient isotope of astatine to date,  $^{190}\text{At}$ , were studied successfully. Additionally, two candidate events were recorded for the heaviest proton emitter observed to date,  $^{188}\text{At}$ . The isotopes were produced in a fusion-evaporation reaction using  $^{\text{NAT}}\text{Ag}$  target and  $^{84}\text{Sr}$  beam with energies between  $\sim 355 - 380$  MeV (c.o.t). The experiment was carried out in JYFL Accelerator laboratory using the K-130 cyclotron and RITU (Recoil Ion Transport Unit) gas-filled separator. The measured values for  $^{190}\text{At}$   $\alpha$ -decay properties were an  $\alpha$ -particle energy of 7750(20) keV and a half-life of  $1.0^{+1.4}_{-0.4}$  ms. The measured properties were analysed and the same spin and parity as the final state ( $10^-$ ) is suggested, since the decay was calculated to be unhindered. Moreover, there are two events that correspond to the proton and  $\alpha$  emission from  $^{188}\text{At}$ . The decay properties of this proton emitter were studied as well, and the measured proton-emission energy was 1500(40) keV and the half-life  $190^{+350}_{-80}$   $\mu\text{s}$ . The measured values are compared to the theoretical predictions, and to the systematics of the neighboring nuclei, in which they fit well.

Keywords: Master's Thesis, nuclear physics, new isotope, astatine, nuclear spectroscopy



## Tiivistelmä

Kokkonen, Henna

Uusien  $^{188}\text{At}$  ja  $^{190}\text{At}$  isotooppien hajoamisominaisuudet

Pro gradu -tutkielma

Fysiikan laitos, Jyväskylän yliopisto, 2023, 47 sivua

Tässä Pro Gradu -tutkielmassa tutkitaan uusia astatiinin isotooppeja ja niiden hajoamisominaisuuksia.  $^{190}\text{At}$  isotoopin ominaisuuksia on tutkittu onnistuneesti. Tämän lisäksi mittauksessa havaittiin kaksi tapahtumaa, joiden voidaan arvioida olevan peräisin tähän asti raskaimmasta raportoidusta protonihajoavasta ytimestä,  $^{188}\text{At}$ . Ytimet tuotettiin fuusio-höyrystymisreaktiolla käyttämällä  $^{\text{NAT}}\text{Ag}$  kohtiota ja  $^{84}\text{Sr}$  ionisuihkua energioilla välillä  $\sim 355\text{ MeV}$ - $380\text{ MeV}$  (keskellä kohtiota). Mittaus on toteutettu JYFL Kiihdytinlaboratoriossa käyttämällä K-130 hiukkaskiihdytintä sekä RITU (Recoil Ion Transport Unit) kaasutäytteistä rekyyliseparaattoria.  $^{190}\text{At}$ :lle mitattuja arvoja ovat  $\alpha$ -hiukkasen hajoamisenergia  $7750(20)\text{ keV}$ , sekä puoliintumisaika  $1.0^{+1.4}_{-0.4}\text{ ms}$ . Mitattuja ominaisuuksia tarkasteltiin ja niiden avulla pystyttiin määrittämään muita ominaisuuksia, kuten tilan spin ja pariteetti, joiden ehdotetaan olevan ( $10^-$ ). Tämä perustuu siihen, että ytimen hajoaminen määritettiin sallitaksi  $\alpha$ -hajoamiseksi, jolloin alku- ja lopputilojen spin ja pariteetti pysyvät samana.  $^{190}\text{At}$ :n lisäksi havaittiin yksi tapahtuma, joka vastaa mahdollisesti protonihajoavaa astatiinin ydintä,  $^{188}\text{At}$ . Myös tämän ytimen ominaisuuksia tutkittiin ja ytimen protonihiukkasen hajoamisenergiaksi määritettiin  $1500(40)\text{ keV}$  ja puoliintumisajaksi  $190^{+350}_{-80}\text{ }\mu\text{s}$ . Määritettyjä tuloksia verrattiin teoreettisiin ennustuksiin sekä ympäröivien ytimien systematiikkaan, joihin ne sopivat hyvin.

Avainsanat: Pro Gradu -tutkielma, ydinfysiikka, isotooppi, astatiini, ydinspektroskopia



## Preface

The experimental data analysed in this thesis is from an experiment that was performed in 2005 by the In-beam Spectroscopy group and the JYFL Gas-filled Recoil Separator RITU group of JYFL Accelerator laboratory. Therefore, I did not participate in the experiment, but my part of this work was to analyse the data and write the manuscript with the help from my supervisor when needed. Since there were people participating in the experiment, before submitting the paper to the review, each of the participants were allowed to comment the text from which the needed corrections were made.

The greatest thanks belongs to my supervisor Kalle Auranen for giving me the opportunity to do this study. Kalle has helped me patiently with this project and has taught me a lot. I am grateful for the whole Nuclear Spectroscopy group of the JYFL Accelerator Laboratory for encouraging me during this project and inspiring me to study nuclear physics. I am very glad for the opportunity to follow your work during the past year. I also want to thank my friends and family for the support and encouragement during this thesis process.

Jyväskylä

Henna Kokkonen





# Contents

<b>Abstract</b>	<b>3</b>
<b>Tiivistelmä</b>	<b>5</b>
<b>Preface</b>	<b>7</b>
<b>1 Introduction</b>	<b>11</b>
<b>2 Theoretical background</b>	<b>13</b>
2.1 Nuclei . . . . .	13
2.2 Nuclear shell model . . . . .	14
2.3 $\alpha$ -decay . . . . .	15
2.4 Proton emission . . . . .	17
2.5 Fusion-evaporation reactions . . . . .	18
2.6 Half-life considerations in case of very low statistics . . . . .	19
2.7 Radioactive decay probability . . . . .	20
<b>3 Measurement system</b>	<b>21</b>
3.1 RITU recoil separator . . . . .	21
3.2 Focal plane . . . . .	22
<b>4 Results</b>	<b>25</b>
4.1 $^{190}\text{At}$ . . . . .	25
4.2 Proton decay of $^{188}\text{At}$ . . . . .	25
<b>5 Summary</b>	<b>31</b>
<b>References</b>	<b>31</b>
<b>A Properties of the new <math>\alpha</math>-decaying isotope <math>^{190}\text{At}</math></b>	<b>41</b>



# 1 Introduction

Nuclei and their properties are studied in the physics field of nuclear spectroscopy. The first studies of the atomic nuclei were made over hundred years ago. To date, there are over 3,600 isotopes known [1] and the studies of them are increasing our knowledge of the limits of existing matter. Studies at the limits of known matter are important for determining the nuclear structure and the configurations of nucleons inside the nuclei. Moving towards to the more exotic nuclei, the production yields and half-lives become very small, and the studies require more complex detecting systems and data analyses. However, these nuclei can be studied via  $\alpha$ -decay spectroscopy. It is a very efficient technique, in which it is possible to define the  $\alpha$ -particle energy, half-life, mass excess, and one proton separation energy with only few observed events. With the determined properties some fundamental questions on structure and properties of nuclear matter can be discussed. These questions are, for example, (*i*) location of the proton drip line, (*ii*) the strength of shell closures, and (*iii*) predictive power of atomic mass models. Furthermore, the reduced decay width and the hindrance factor can be calculated and with these, overlap of the wave functions of the initial and final state, and preformation factor can be studied.

Astatine is a very rarely occurring element on Earth, and it is produced as a decay product of uranium ores in the crust of the Earth. At any point of time there is not more than one tablespoon of astatine occurring in the crust due to very short half-lives. Its longest living isotope  $^{210}\text{At}$  has a half-life of only 8 hours, however, longest naturally occurring isotope of astatine  $^{219}\text{At}$  has a half-life of 56 seconds. [2-4] Relatively small amount of astatine data have been measured, and before this study, the most neutron deficient and lightest known astatine isotope is  $^{191}\text{At}$  [5]. The most exotic and neutron-deficient odd-odd nuclei are challenging to study, however, the states of the odd-odd astatine, bismuth, and francium high-spin states are studied before in, for example, Refs. [6-8]. The most neutron deficient isotope of astatine known prior this work is  $^{192}\text{At}$  [9]. Moreover, no proton-emitting astatine isotopes have been observed yet, the heaviest proton-emitting nuclide is  $^{185}\text{Bi}$  [10].

This Master's Thesis is an article-form thesis consisting of two parts, the manuscript: *Properties of the new  $\alpha$ -decaying isotope  $^{190}\text{At}$* , that has been the main focus of this study. Furthermore, more analysis of the measured data is carried out and, additionally, another new isotope is suggested to be found, including a general overview of the concepts of the study. The manuscript (Appendix [A](#)) was submitted to Physical Review C journal, therefore, the article has been written to reach the researchers in the field instead of the audience that is normally reached in Master's Thesis. Therefore, the first part (Sections [1-3](#)) of this work is a brief introduction to the concepts of the article to accomplish wider audience for the thesis. Additionally, in Section [4.2](#) the data measured in the experiment are analysed more and the indications of a heavy proton-emitting isotope  $^{188}\text{At}$  are discussed and presented.

## 2 Theoretical background

The following section is an overview of some of the important concepts discussed in this thesis. Additionally, the aim is to provide a better understanding of the observations and conclusions made in the article (Appendix [A](#)).

### 2.1 Nuclei

Nucleons, protons ( $p$ ) and neutrons ( $n$ ), are particles that compose atomic nuclei which are affected by different nuclear forces. These are the attractive strong interaction, and the weak interaction, and the repulsive Coulomb force. The strong interaction affects between the nucleons to hold the nucleus together, whereas the weak interaction appears inside the nucleons. The Coulomb force is an interaction between the positive charges, protons. The Coulomb force between two particles is

$$F_C = \frac{1}{4\pi\epsilon_0} \frac{q_1 q_2}{r^2},$$

where  $\epsilon_0$  is the electric constant,  $q_1$  and  $q_2$  are the charges of the particles, and  $r$  is the distance between the particles.

Each nuclear species has its own mass number  $A$ , which indicates the number of nucleons in the nucleus. The simplest atom, hydrogen  $^1\text{H}$ , consists of a proton and an electron. The proton is the fundamental positively charged particle inside the nucleus, and therefore the number of protons  $Z$  determines the element. [\[11\]](#) However, there exist many nuclei with the same proton number but different mass and neutron numbers, these are called isotopes. All known isotopes are organized to nuclide chart based on their proton and neutron numbers, see Fig. [1](#), and, for example Ref. [\[12\]](#).

Atomic nuclei can be classified by their properties as stable and unstable nuclei. Moving towards more exotic neutron or proton deficient nuclei in the nuclear chart, finally a drip line is reached. The drip line is located on the nuclear chart at both, proton and neutron separation energy of 0. In this study, the nuclei over the proton drip line are studied, therefore, it will focus on the proton drip line and proton-

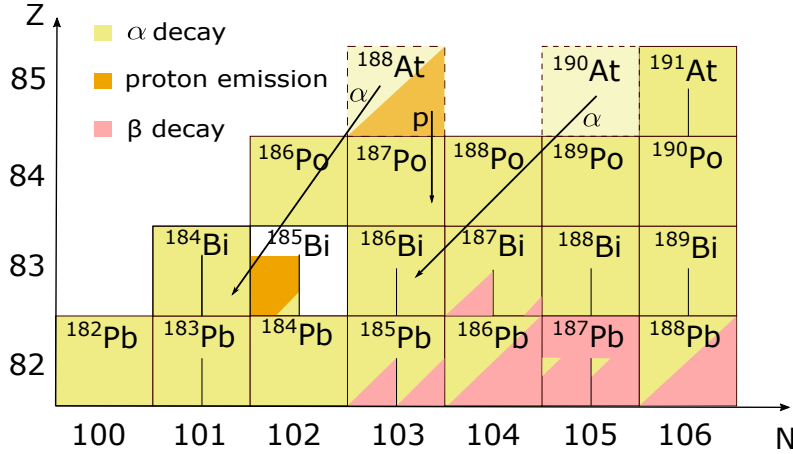


**Figure 1.** Schematic of the nuclear chart on the neutron deficient nuclei around  $82 \leq Z \leq 85$ , and  $100 \leq N \leq 106$ . The isotopes studied in this study are expressed in dashed lines and lighter colors. The proton decay and  $\alpha$ -decay paths from the observed nuclei are marked with arrows. The blocks marked on white are not discovered yet. [12]

separation energy,  $S_p$ , instead of neutrons. As the separation energy is less than zero, proton cannot bind to the nucleus. However, there are observed heavy and exotic nuclei beyond the proton-drip line, which are held together by a barrier arising from the combined effect of the strong, Coulomb and centrifugal components. Eventually protons will tunnel through the barrier. [13]

## 2.2 Nuclear shell model

Different models have been proposed to improve the understanding of the nuclear structures and how the nucleons are placed inside the nucleus. The shell model [14] suggests that the structure of a nucleus is analogous to the electron shell structure of an atom. At major shells of nuclei, also referred to as the magic numbers ( $N$  or  $Z = 2, 8, 20, 28, 50, 82, \dots$ ), locates the local maxima of the separation energies, therefore, by observing the proton and neutron separation energies one can probe the shell structure as well.

The charges oscillating in the nuclei produce an electromagnetic field. The charges and currents transmit energy and angular momentum, which must be conserved in the system. The angular momentum originates from individual nucleons moving orbitally and from the intrinsic spin of the nucleons. [15] Nucleons can occupy different energy levels inside the nucleus, and subshells are labeled by the angular

momentum  $l$  of the nucleon: s, p, d, f, g, h for  $l = 0, 1, 2, 3, 4, 5$ , respectively. The angular momentum is the central potential of the nucleon moving inside the nucleus, the spin quantum number  $s$  is  $1/2$  for the nucleons. The total angular momentum can be then written as

$$\mathbf{j} = \mathbf{l} + \mathbf{s}.$$

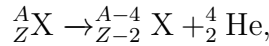
The interaction between the spin orbits can be described as

$$V_{so}(r)\langle l \cdot s \rangle = V_{so} \frac{1}{2} [j(j+1) - l(l+1) - s(s+1)] \hbar^2. \quad (1)$$

Here  $V_{so}$  is the potential strength between the neighbouring nucleons. By adding the spin-orbit term to the Woods-Saxon potential, and by solving the Schrödinger equation, one can evaluate the sequence in which the different orbitals are filled [11]

### 2.3 $\alpha$ -decay

Elements beyond the lead region ( $Z \geq 82$ ) are observed to decay mainly via  $\alpha$  decay.  $\alpha$  decay is a reaction where the nucleus emits an  $\alpha$  particle.  $\alpha$  particle has the structure of  ${}^4\text{He}$  nucleus, consisting of two protons and two neutrons. The decay can be expressed as



where number of protons  $Z$  defines the element X.

The binding energy released in the  $\alpha$  decay is equal to the mass lost in the reaction and, therefore, can be calculated using the atomic masses  $m$  of the decay products. [15] This is also known as the  $Q$  value of  $\alpha$  decay and can be defined as

$$Q_\alpha = -u\Delta M = -u \cdot [m_i - m_d - m_\alpha], \quad (2)$$

where  $m_i$ ,  $m_d$ , and  $m_\alpha$  are the masses of the initial nucleus, the daughter nucleus, and the emitted  $\alpha$  particle, respectively. The constant  $u$  is the atomic mass unit equal to  $931.5 \text{ MeV}/c^2$ . When nucleus undergoes a decay from the ground state to the ground state, the energy is shared by kinetic energies of the reaction products,  $\alpha$  particle and the daughter nucleus. [15, 16] As the energy is conserved, the  $Q_\alpha$  value can be derived using the kinetic energy of the  $\alpha$  particle  $E_\alpha$ , and the masses of the

decay products,

$$Q_\alpha = E_\alpha \left(1 + \frac{m_\alpha}{m_d}\right). \quad (3)$$

The rate of which the  $\alpha$  particles are emitted can be predicted by using the probability of an  $\alpha$  particle to tunnel through Coulomb barrier and the probability of an  $\alpha$  particle to appear inside the nucleus. Therefore, the particle emission rate can be expressed as a partial decay constant  $\lambda$ ,

$$\lambda = \frac{dP}{dt} = fT, \quad (4)$$

that is the decay probability  $P$  by time  $t$ , that equals to the product of the frequency factor  $f$  and the transmission coefficient  $T$ . [16] Using the partial decay constant, the half-life of a nucleus can be deduced

$$t_{1/2} = \frac{\ln(2)}{\lambda} = \tau \ln(2), \quad (5)$$

where the  $\tau$  is the mean lifetime, and half-life  $t_{1/2}$  is the time that it takes for a sample of a given isotope to decay to half of the initial amount.

The  $\alpha$  emission of the nucleus can be estimated by observing the Coulomb-barrier penetration of the  $\alpha$  particle, illustrated in Fig. 2. By studying the  $\alpha$  scattering and deriving the nuclear potential, the barrier-penetration factor  $P$  can be calculated using the WKB integral,

$$\ln(P) = -2 \int_{R_i}^{R_o} \frac{(2M)^{1/2}}{\hbar} \left[ V(r) + \frac{2Ze^2}{r} + \frac{\hbar^2}{2mr^2} l(l+1) - E \right]^{1/2} dr. \quad (6)$$

Here  $\hbar$  is the reduced Planck constant,  $M$  the reduced mass of the  $\alpha$  particle,  $V(r)$  is the  $\alpha$ -nuclear potential as a function of distance  $r$ ,  $Ze$  is the daughter nucleus charge, and  $l$  is orbital angular momentum of the emitted  $\alpha$  particle. Finally,  $E$  is the sum of the  $\alpha$ -particle, recoil, and electron-screening energies, which is equal to the total decay energy. [17] Using the penetration factor and the decay constant, one can derive a reduced  $\alpha$ -emission width  $\delta^2$  of the decay from the following equation,

$$\lambda = \frac{\delta^2 P}{h}, \quad (7)$$

where  $h$  is the Planck constant [17]. The reduced  $\alpha$ -emission width is proportional



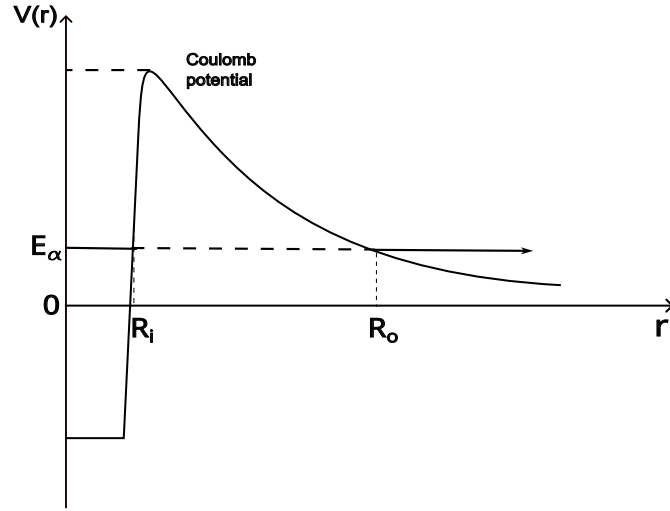


**Figure 2.** An  $\alpha$  particle tunneling through the Coulomb barrier as a function potential and atomic radius.  $R_i$  is the inner radius and  $R_o$  the outer radius. [11]

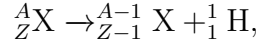
to the decay constant and, therefore, to the penetration probability of the  $\alpha$  particle and the half-life of the decay, see Eq. [5]. The relationship between the experimental and theoretical values of the half-lives can be examined to derive a hindrance factor  $HF$  of the decay. The hindrance factor can be used to consider the state of the initial and final states of the decay. [18] With  $HF < 4$ , the  $\alpha$  decay is said to be unhindered, and the involved initial and final states likely have the same spin and parity.

## 2.4 Proton emission

The properties of proton emission are rather similar to those of  $\alpha$  decay. However, in the following section, some essential properties for understanding the possible observation of proton-emitting nucleus are introduced.

Coulomb barrier for proton emission is half that of the  $\alpha$  decay, however, only approximately 50 cases of proton emission are known between ionide ( $Z = 53$ ) and bismuth ( $Z=83$ ) [19]. The process can rarely compete with other decay processes. For majority of the known nuclei the proton-decay Q-value is negative making the decay energetically forbidden. Beyond the proton dripline the emission is energetically possible, however, when moving towards the even more exotic nuclei the increasing Q-value quickly makes the decay too fast to be observed with the available experimental

techniques. The proton emission can be expressed as,



and its path in the nuclear chart is expressed in Fig. [1](#) [\[11\]](#)

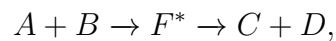
If proton-particle energy  $E_p$ , mass of the proton  $m_p$  and product nucleus  $m_d$  are known, the Q value for proton decay can be deduced analogous way as for  $\alpha$  decay in Eq. [3](#),

$$Q_p = -u\Delta M = E_p \left(1 + \frac{m_p}{m_d}\right). \quad (8)$$

Here the decay is assumed to occur from ground state to ground state. The principles of the proton decay is similar to those of  $\alpha$  decay, and half-life can be obtained using Eq. [5](#).

## 2.5 Fusion-evaporation reactions

Fusion-evaporation reaction is one of the ways to produce exotic nuclei, particularly on the neutron deficient side of the chart of nuclides. As a result of the reaction, also very rare and short living nuclei can be produced. In fusion-evaporation reaction target is irradiated using an accelerated ion beam. The reaction produces a nucleus of the fusion compound. The compound nucleus then rapidly emits lighter particles, for example, protons, neutrons, or  $\alpha$  particles,



which can be expressed as



Here,  $A$ ,  $B$ ,  $C$ , and  $D$  are the target, projectile, emitted particles and daughter nucleus, respectively and  $F^*$  is the compound nucleus. The fusion-evaporation reaction often produces a variety of some dozens of nuclei, depending on the target, beam, and energy of the incident particle. To obtain the desired nuclei these properties must be chosen carefully. [20](#) Simplified illustration of the fusion-evaporation reaction is presented in Fig. [3](#). The most favorable particles to be evaporated are neutrons, since they do not need to overcome the Coulomb barrier when they are emitted from

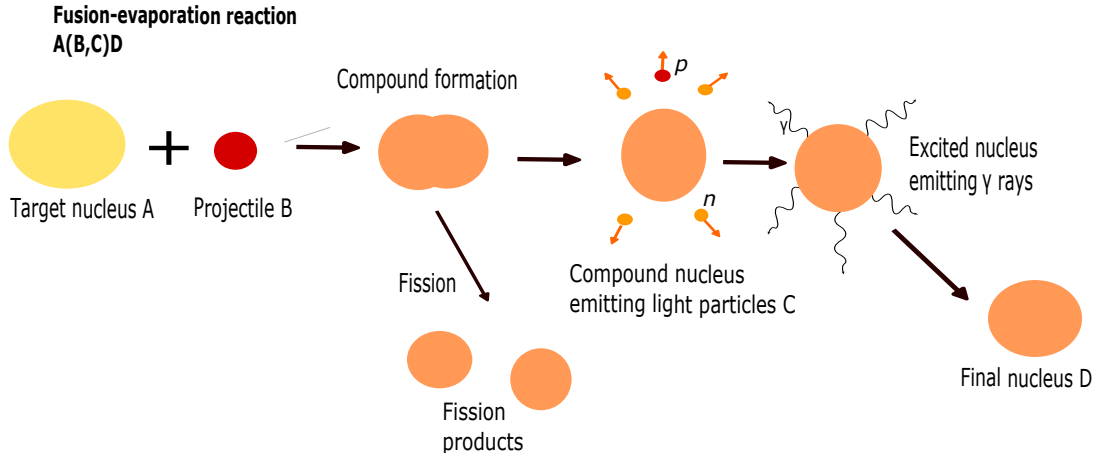


**Figure 3.** Schematic of fusion-evaporation reaction. As the projectile hits the target nucleus, it forms a compound nucleus, which then emits particles to form the final product. The reaction products are still in excited state, which then emits  $\gamma$  rays to de-excite and reach ground state or low-lying isomeric state.

the compound nucleus. Therefore, neutrons are the first particles to be emitted in the process. The emission of particles reduces the excitation energy of the compound nucleus. This is due to the kinetic energies of the evaporated particles and the separation energies. The evaporation of particles continues until the excitation energy of the compound nucleus falls below the particle-separation energy. As visualized in Fig. 3, after the compound nucleus has evaporated all the particles, it reaches an excited state, and the decay continues via  $\gamma$ -ray emission until the ground state or a low-lying isomeric state of the nucleus is reached. [21]

## 2.6 Half-life considerations in case of very low statistics

The maximum likelihood estimate is an approximation for lifetimes of a nuclear species. Better accuracy for small number of events can be reached, compared to the ones done using the standard deviation. The mean lifetime  $\tau$  is taken to be the arithmetic mean of the individual events  $(t_m)_i$ ,

$$\tau = \frac{1}{n} \sum_{i=1}^n (t_m)_i, \quad (9)$$

where  $n$  is the number of events. When number of events is greater than two, the lower and upper confidence limits  $\tau_{l,u}$  of the lifetime can be calculated with

approximation,

$$\tau_l \approx \frac{\overline{t_m}}{1 - z/\sqrt{n}}, \quad \tau_u \approx \frac{\overline{t_m}}{1 + z/\sqrt{n}}. \quad (10)$$

Here  $z$  is a quantity related to confidence level, that is in this study  $z = 1$ . [22]

## 2.7 Radioactive decay probability

When observing multiple decay sequences, the origin of the chains can be evaluated using, for example, Schmidt's radioactive decay probability test [23]. The test evaluates the probability of the decay chain to originate from a single radioactive species. The decay data are distributed by the density of the decay time, as  $\ln(t) = \Theta$ ,

$$\left| \frac{dn}{d\Theta} \right| = n_0 \exp(\Theta + \ln \lambda) \exp(-\exp(\Theta + \ln \lambda)). \quad (11)$$

From the density distribution curve, the maximum of the curve  $\Theta_{\max}$  is

$$\frac{d^2n}{d\Theta^2} = 0 \rightarrow \Theta_{\max} = \ln \frac{1}{\lambda}. \quad (12)$$

The curve of the decays is slightly asymmetric-shaped, and using it one can test whether a second decay contributes the spectrum. The standard deviation for the measured decay times can be calculated with the following equation,

$$\sigma_{\Theta_{\exp}} = \sqrt{\frac{\sum_{t=1}^n (\Theta_i - \overline{\Theta}_{\exp})^2}{n}}. \quad (13)$$

Here  $\overline{\Theta}_{\exp}$  equals the mean value of the measured decay times  $\Theta_i$  and  $n$  the number of events:

$$\overline{\Theta}_{\exp} = \frac{\sum_{t=1}^n \Theta_i}{n}. \quad (14)$$

The standard deviation limits for each number of events have been calculated numerically. If the standard deviation fits inside the limits, the decays can be assumed to origin from the single radioactive species with a probability greater than 90 %. [23]

### 3 Measurement system

The experiment was carried out in the JYFL accelerator laboratory. The system is presented briefly in the article, Appendix [A](#). However, this section is a more detailed overview of the experimental setup used in the experiment which was carried out to produce the observed new isotopes.

#### 3.1 RITU recoil separator

The produced recoils are separated in-flight from other particles, such as fission products, target-like, and beam-like particles, using RITU (Recoil Ion Transport Unit [\[24, 25\]](#)) gas-filled recoil separator. RITU uses magnetic rigidity of the particles to separate the beam from the produced recoils. The magnetic rigidity  $B\rho$  is expressed as a product of the magnetic field strength  $B$  and the radius of curvature  $\rho$

$$B\rho = \frac{p}{q} \approx \frac{mv}{q}, \quad (15)$$

where  $p$  is the momentum and  $q$  is the equilibrium charge of the reaction products.

The separator is filled with helium gas to 1 mbar pressure, and has an ion-optical configuration of QDQQ. That is, RITU consists in total of three quadrupoles Q and one dipole D, see Fig. [4](#). The first quadrupole after the target chamber improves the angular acceptance of the dipole by focusing the products vertically. The dipole is followed by two focusing quadrupoles. Gas-filled separators have high transmission, which is useful for studies with low production rates. The filling gas interacts with the recoils and, therefore, the products change their charge state frequently as they fly in the separator. Consequently, the products follow the trajectory of an average charge state, which needs to be evaluated semi-empirically. [\[26-28\]](#)

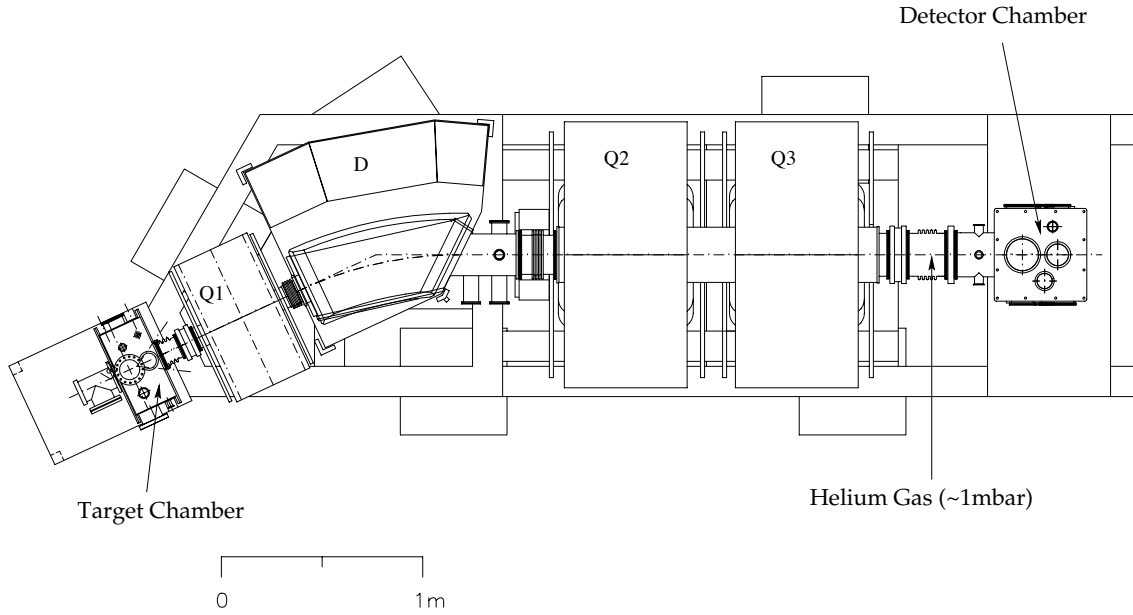


**Figure 4.** Schematic figure of RITU. The separator is filled with helium gas in 1 mbar pressure, the target chamber is located at the beginning of the RITU (left) and detector chamber at the focal plane (right). The optical configuration of the separator is presented as Q1DQ2Q3, where the Q stands for quadrupoles and D for dipole. [24, 25] The figure is taken from [29].

### 3.2 Focal plane

The produced recoils are transported to the focal plane of RITU, where the recoils are observed, in approximately  $1 \mu\text{s}$  after their production in the target chamber. GREAT (Gamma Recoil Electron Alpha Tagging [30]) spectrometer is located at the focal plane. The detectors used in the present study were a multiwire proportional counter (MWPC), a double-sided silicon strip detector (DSSD), and a planar germanium detector. A simplified schematic of the detector components at the focal plane is presented in Fig. 5.

The function of the detector setup is to distinguish the recoils and decay products from target-like and beam-like particles. This is done by using MWPC and Planar Germanium detectors as veto detectors. Planar is a double-sided germanium strip detector for low-energy  $\gamma$  ray and X ray detection, but it is also sensitive for charged particles. The first detector that particles hit when entering to the GREAT is MWPC. The MWPC is filled with isobutane, which is separated from the separator pressure using thin Mylar foils, and is used to detect the energy loss of the charged particles. The particles ionize the gas and release electrons and ions, which are then

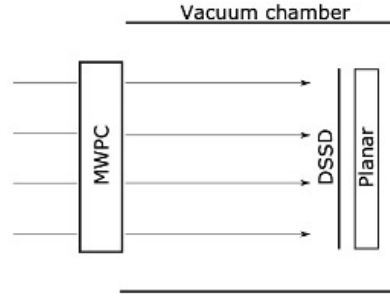


**Figure 5.** The schematic of the GREAT spectrometer components at RITU focal plane.

collected to the anode and cathode wires. The produced recoils are separated from unwanted particles by measuring the energy loss in MWPC and the time of flight between DSSD and MWPC. DSSD is the detector used to implant and measure the recoils and the decay products. The DSSD setup used in the experiment consisted of two DSSDs next to each other to increase the area in which the particles are measured. Each detector had 60 horizontal and 40 vertical strips, each 1 mm wide. The thickness of the DSSD was 300  $\mu\text{m}$ . The calibration of the DSSD was performed with the  $\alpha$  activities of  $^{78}\text{Kr} + ^{92}\text{Mo}$  reaction. The used  $\alpha$ -energy peaks were  $^{150}\text{Dy}$ ,  $^{162}\text{W}$ ,  $^{163}\text{W}$ ,  $^{166}\text{Os}$ ,  $^{167}\text{Os}$ , and  $^{167m}\text{Ir}$  [31–35], these activities are well known and, therefore, are suitable for the calibration.

The detection of the recoil particles and their decay events was done using the DSSD. The event was counted as a decay event only when the particle did not leave a signal in the MWPC nor in the Planar. Moreover, the  $\alpha$  particles correlating with the decaying recoil must be measured in the same pixel of the DSSD, and the first decay product must occur in 10 ms from the recoil implantation. Occasionally, the decay products can escape the DSSD by leaving only part of their energy to the pixel, or the decay can occur during the dead time of the detector. The dead time is an interval of time in which the counts cannot be separated from each other.

As the particle leaves energy to the detector a charge is created, amount of which is proportional to the energy. The charge is then transferred to a pre-amplifier, which converts the detector's current signal into the voltage step signal, which is then transferred to shaping amplifier. The shaped, semi-Gaussian signal is then guided to ADC (Analog to Digital Converter) and the data are analysed with computer programs. In this thesis, the GRAIN [36] software package was used for the data analyses.





## 4 Results

### 4.1 $^{190}\text{At}$

The new astatine isotope was produced and its properties were presented in the article published as part of this thesis, see Appendix [A](#). The  $\alpha$ -decay properties, such as  $\alpha$ -particle energy and half-life, were identified, as well as the possibility to proton decay was discussed.

### 4.2 Proton decay of $^{188}\text{At}$

In addition to the new  $^{190}\text{At}$  isotope, there are two observed candidate events for the heaviest proton-emitting isotope observed so far. One of the events is a proton decay event, whereas the other is an  $\alpha$ -decay event with only partially recorded energy. However, to publish the new isotope, more decay chains should be observed. As there are only the mentioned two candidate events for the new isotope, it is not presented in the article.

The target used in the experiment was natural silver target, that is a mixture of  $^{107}\text{Ag}$  and  $^{109}\text{Ag}$ . The abundances for the isotopes are 52% and 48%, respectively [\[12\]](#). As the  $^{190}\text{At}$  was produced in the fusion-evaporation reaction  $^{109}\text{Ag}(^{84}\text{Sr},3\text{n})^{190}\text{At}$ , the  $^{188}\text{At}$  was produced in  $^{107}\text{Ag}(^{84}\text{Sr},3\text{n})^{188}\text{At}$  reaction. The calibration for lower energies was performed using the same calibration measurement as before, yet the proton-emission peaks were used. The used peaks were  $^{166}\text{Ir}$ ,  $^{166\text{m}}\text{Ir}$ ,  $^{167}\text{Ir}$ , and  $^{167\text{m}}\text{Ir}$  [\[37, 38\]](#).

There are two candidates for the decays of  $^{188}\text{At}$  observed in this study, a proton decay and an  $\alpha$  decay, see Fig. [6](#). The proton decay of  $^{188}\text{At}$  is observed with a decay chain  $^{188}\text{At} \xrightarrow{p} ^{187}\text{Po} \xrightarrow{\alpha} ^{183}\text{Tl} \xrightarrow{\alpha} ^{179}\text{Hg}$ . The observed  $\alpha$  particle of the  $\alpha$  decay was not recorded with its full energy, since occasionally the particles can escape the detectors leaving only part of their energy to it. Nevertheless, the observed candidate  $\alpha$ -decay sequence is  $^{188}\text{At} \xrightarrow{\alpha} ^{184}\text{Bi} \xrightarrow{\alpha} ^{180}\text{Tl} \xrightarrow{\beta+/EC} ^{180}\text{Hg} \xrightarrow{\alpha} ^{176}\text{Pt}$ . Due to the escaped  $\alpha$  particle, the  $\alpha$  decay of  $^{188}\text{At}$  cannot be studied directly. However,

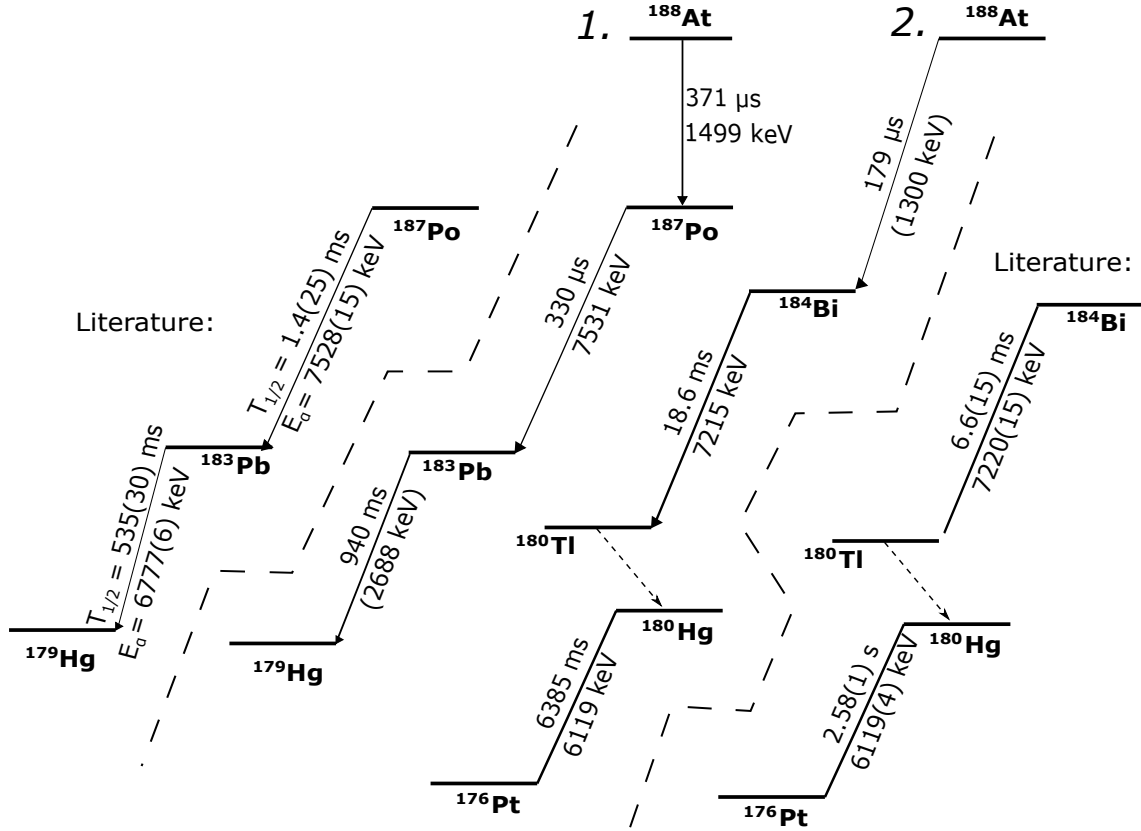


**Figure 6.** The energies and half-lives of the decay chain for the proton decaying  $^{188}\text{At}$  (1.) observed in the experiment. Additionally, an  $\alpha$ -decay event (2.) observed is presented. The literature values are expressed above and below the dashed lines [39–42]. Energies marked in parentheses indicate the energies of  $\alpha$  particles that escaped from the DSSD and therefore full energies were not measured. The  $^{182}\text{Tl} \rightarrow ^{182}\text{Hg}$  step remains unobserved as well, since the DSSD is insensitive to electron capture and  $\beta^+$  decay.

the observed decaytime fits to the one observed from the proton emission, and can be taken into account when determining the half-life of the  $^{188}\text{At}$ .

The energy released in the proton emission is

$$E_p = 1500(40) \text{ keV.}$$

Since there is only one proton emission event observed, the error analysis of the deduced proton-particle energy was derived from the FWHM (Full Width at Half Maximum) of the DSSD. Using the arithmetic mean (9) of the observed two events, the mean lifetime of the nuclide is  $\tau = 275 \mu\text{s}$ , from which the half-life can be

**Table 1.** The values [1] of the nuclear masses and mass excesses needed for the calculations to derive the decay properties of the  $^{188}\text{At}$ .

	Atomic mass (MeV/c <sup>2</sup> )	Mass excess (keV)
proton	1.00782503190(1)	7288.97106(1)
$\alpha$	4.00260325413(15)	2424.91587(16)
$^{184}\text{Bi}$	184.001350(130)	1250(120)
$^{187}\text{Po}$	187.003030(30)	2820(40)

obtained with Eq. (5),

$$t_{1/2} = 190 \mu\text{s}.$$

The uncertainty analysis was carried out by taking into account the statistics and calculating the errors with standard errors for  $n = 2$  as described in Ref. [22]. The lower and upper limits of the mean lifetime for  $n = 2$  these are  $0.606\tau$  and  $2.82\tau$ , respectively [22]. Therefore, the result for the half-life of the nuclide is  $t_{1/2} = 190_{-80}^{+350} \mu\text{s}$ . The proton-decay  $Q$ -value for the present decay can be calculated with Eq. (8), as the proton-particle energy is obtained above and the masses of proton and  $^{187}\text{Po}$  are presented in Table [1].

$$Q_p = 1510(40) \text{ keV}.$$

The state from which the proton is emitted can be estimated by the systematics of surrounding nuclei. The possible states are  $s_{1/2}$ ,  $f_{7/2}$  and  $h_{9/2}$ . These can be evaluated by using the proton decay  $Q$ -value and the WBK integral to calculate the theoretical partial half-lives of different states and to compare those with the measured results. With the measured  $Q_p$  the partial half-lives for states  $s_{1/2}$ ,  $f_{7/2}$  and  $h_{9/2}$  are  $44 \mu\text{s}$ ,  $1.6 \text{ ms}$ , and  $510 \text{ ms}$ , respectively. When comparing the obtained half-life, it can be suggested, that the proton is emitted from the  $s_{1/2}$  state. For this state the calculated partial half-life is the closest to the measured one. This conclusion is supported by the systematics, since in  $^{185}\text{Bi}$  the proton is emitted from the  $s_{1/2}$  state as well [10]. Moreover, another possible state is  $f_{7/2}$ , in which the measured half-life fits inside the error limits. To draw more precise conclusions, more statistics would be required.

For a better understanding of the reliability of the observation, the obtained values are compared with theoretical predictions and systematics of nearby nuclei.

**Table 2.** The decay properties of  $^{188}\text{At}$  obtained in this study.

Quantity	Obtained value
$t_{1/2}$	$190_{-80}^{+350} \mu\text{s}$
$E_p$	1500(40) keV
$Q_p$	1510(40) keV
$E_\alpha$	7800(200) keV
$Q_\alpha$	7900(200) keV

Observed proton emission can be used to obtain information of a possible  $\alpha$  decay of the new  $^{188}\text{At}$  isotope and the  $\alpha$ -decay properties can be extracted.

From the proton emission  $Q$ -value calculated above, the mass excess of the new nucleus can be derived from Eq. (8) using the values displayed in Table 1,

$$\Delta M(^{188}\text{At}) = Q_p + \Delta M(\text{p}) + \Delta M(^{187}\text{Po}) = 11600(300) \text{ keV}.$$

The  $\alpha$ -decay properties of the presently observed isotope can be considered from the measured properties and compared to the systematics of the nearby nuclei and mass-model predictions. Using the mass excess and the values from Table 1, also the  $Q_\alpha$  value for the  $\alpha$  decay of the new isotope can be calculated,

$$Q_\alpha = 7900(200) \text{ keV}.$$

With the deduced decay energy, the  $\alpha$ -particle energy can be derived and calculated from Eq. (3)

$$E_\alpha = 7800(200) \text{ keV}. \quad (16)$$

The uncertainty analysis of the derived values was calculated using standard error. The results obtained are expressed in Table 2.

The hindrance factor  $HF$  of the decay is calculated to be 0.4, which refers to an unhindered decay. The factor is calculated with the equations (6) and (7). Since there was one observed event of both  $\alpha$  decay and proton emission,  $HF$  was calculated by assuming an  $\alpha$ -decay branch of 50 %. The normalization of  $\delta^2(^{188}\text{At})$  to  $\delta^2(^{212}\text{Po})$  was done by using the properties of  $\alpha$ -decay of  $^{212}\text{Po}$  [43].  $^{212}\text{Po}$  is a nuclide which  $\alpha$  decay to doubly magic  $^{208}\text{Pb}$  and is therefore a good reference nuclide.

In Fig 7, the deduced  $\alpha$ -decay energy of presently observed  $^{188}\text{At}$  is compared with systematics of neighbouring odd-odd nuclei of astatine and bismuth. The

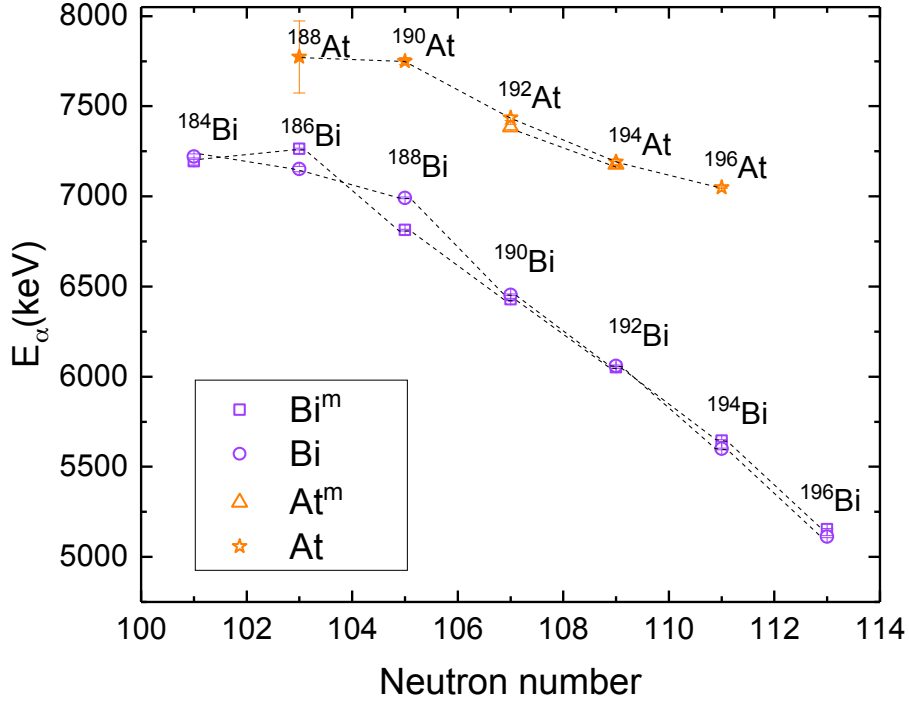


**Figure 7.** The systematics of the measured  $\alpha$ -decay energies of the most exotic neutron-deficient nuclei with odd  $N$  of astatine and bismuth. The values obtained in this thesis are marked as solid symbols, as the rest of the values are obtained from literature. [41, 53–58] The dashed line is an interpolation to improve the readability.

values obtained in this study are marked with solid symbols. The systematics of the lightest astatine isotopes appear to follow that of the nearby bismuth isotopes, as the  $\alpha$ -particle energy is bend down for the more exotic, neutron-deficient nuclei. Additionally, the  $Q_{\alpha}$  value is compared with chosen mass models in Fig. 8. The predicted values from selected mass models are from EDF (UNEDF0 [44], UNEDF1 [45], SkM\* [46], SkP [47], SLy4 [48], and SV-min [49]) obtained from The Mass explorer interface [50], FRDM (2012) [51], and Liran-Zeldes [52]. It can be seen that the obtained value for  $^{188}\text{At}$  fits to the value of FRDM well inside its error limits, as well as for  $^{190}\text{At}$ . Moreover, the FRDM predicts the bending in the  $Q_{\alpha}$  value, which supports the observations made in this study. The EDF does not provide the values of the most exotic odd-odd astatine nuclei, however, the interpolation to the values of even- $N$  isotopes is close to that obtained in this thesis. Moreover, Liran-Zeldes model does not fit for the most exotic nuclei with neutron number less than 109.

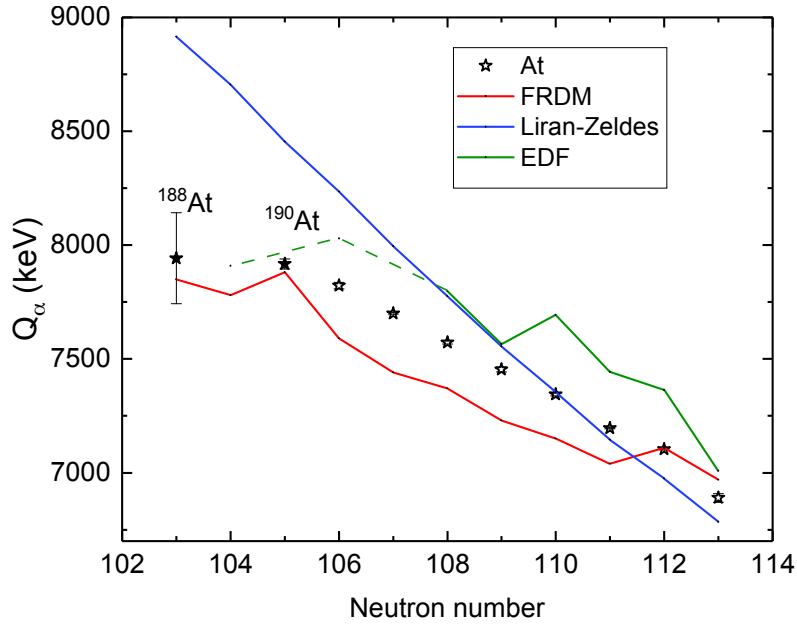


**Figure 8.** The  $Q_\alpha$  values for astatine isotopes measured in this experiment (indicated as solid symbols) compared with different mass model predictions (solid lines) and experimental values measured in other experiments (open symbols). The selected mass model predictions are EDF (UNEDF0 [44], UNEDF1 [45], SkM\* [46], SkP [47], SLy4 [48], and SV-min [49]) obtained from The Mass explorer interface [50], FRDM(2012) [51], and Liran-Zeldes [52]. Experimental data other than that of this work is from AME2020 [1]. The interpolation is indicated with dashed line for EDF, since it does not provide the data for the odd-odd nuclei with neutron number less than 109.

## 5 Summary

In this thesis a new isotope of astatine  $^{190}\text{At}$ , and a candidate events for  $^{188}\text{At}$  are produced and identified. Of these,  $^{190}\text{At}$  is identified with certainty and three  $\alpha$ -decay events of the new isotope are observed. The measured values for the isotope are  $\alpha$ -particle energy of 7750(20) keV and half-life of  $1.0_{-0.4}^{+1.4}$  ms. From these values, more properties of the nuclide are identified. The  $^{190}\text{At}$   $\alpha$  decay was concluded to be unhindered. Consequently, for the  $\alpha$ -decaying state the same spin and parity of ( $10^-$ ) can be proposed as that of the final state of the decay. The possibility of the observed nuclide to emit protons was also considered, however, it was concluded to be unable to compete with the observed  $\alpha$  decay.

The possible observation of proton emitting  $^{188}\text{At}$  was studied. The proton emission was observed to have a particle energy of 1500(40) keV, and a half-life of  $190_{-80}^{+350}$   $\mu\text{s}$ . Similarly to the  $^{190}\text{At}$ , using the measured values, different decay properties were calculated: for example, the possible  $\alpha$ -decay properties were compared to the systematics and the predicted values. Only one event of proton emission increases the uncertainty, and to obtain more precise properties, more events would be required. However, the deduced values for both new isotopes matched well with the theoretically predicted values and systematics, and a new isotope  $^{190}\text{At}$  was identified verifiably, while  $^{188}\text{At}$  was considered. Therefore, the goal of this study was achieved successfully.

It could be possible to study the  $^{188}\text{At}$  more precisely and to produce more events of the isotope if a new experiment would be carried out. This is due to the improved ECR ion sources at the JYFL Accelerator Laboratory, which provides more beam and, therefore, increases the production rate. Additionally, the detection system has been improved since the experiment was carried out. The size of the DSSD is increased and new detectors can be used to detect, for example, the escaped  $\alpha$  particles. These improve the detection of the produced recoils and, therefore, by repeating the experiment, it could be possible to observe more events for the  $^{188}\text{At}$ .





## References

- [1] M. Wang et al. “The AME 2020 atomic mass evaluation (II). Tables, graphs and references\*”. *Chinese Physics C* 45.3 (Mar. 2021). URL: <https://dx.doi.org/10.1088/1674-1137/abddaf>.
- [2] T. Řezanka and K. Sigler. “Biologically Active Compounds Of Semi-Metals”. In: *Bioactive Natural Products (Part O)*. Ed. by Atta-ur-Rahman. Vol. 35. Studies in Natural Products Chemistry. Elsevier, 2008, pp. 835–921. DOI: [https://doi.org/10.1016/S1572-5995\(08\)80018-X](https://doi.org/10.1016/S1572-5995(08)80018-X).
- [3] B. Singh et al. “Nuclear Data Sheets for A = 215”. *Nuclear Data Sheets* 114.12 (2013), pp. 2023–2078. ISSN: 0090-3752. URL: <https://doi.org/10.1016/j.nds.2013.11.003>.
- [4] F. Kondev. “Nuclear Data Sheets for A = 206”. *Nuclear Data Sheets* 109.6 (2008), pp. 1527–1654. ISSN: 0090-3752. URL: <https://doi.org/10.1016/j.nds.2008.05.002>.
- [5] H. Kettunen et al. “Alpha-decay studies of the new isotopes  $^{191}\text{At}$  and  $^{193}\text{At}$ ”. *Eur. Phys. J. A* 17 (Aug. 2003), pp. 537–558. URL: <https://doi.org/10.1140/epja/i2002-10162-1>.
- [6] M. Huyse et al. “Isomers in three doubly odd Fr-At-Bi  $\alpha$ -decay chains”. *Phys. Rev. C* 46 (4 Oct. 1992), pp. 1209–1217. DOI: [10.1103/PhysRevC.46.1209](https://doi.org/10.1103/PhysRevC.46.1209). URL: <https://link.aps.org/doi/10.1103/PhysRevC.46.1209>.
- [7] P. Van Duppen et al. “Intruder states in odd-odd Tl nuclei populated in the  $\alpha$ -decay of odd-odd Bi isotopes”. *Nuclear Physics A* 529.2 (1991), pp. 268–288. ISSN: 0375-9474. DOI: [10.1016/0375-9474\(91\)90796-9](https://doi.org/10.1016/0375-9474(91)90796-9). URL: <https://www.sciencedirect.com/science/article/pii/0375947491907969>.
- [8] J. Uusitalo et al. “ $\alpha$ -decay studies of the francium isotopes  $^{198}\text{Fr}$  and  $^{199}\text{Fr}$ ”. *Phys. Rev. C* 87 (6 June 2013), p. 064304. DOI: [10.1103/PhysRevC.87.064304](https://doi.org/10.1103/PhysRevC.87.064304). URL: <https://link.aps.org/doi/10.1103/PhysRevC.87.064304>.

- [9] A. N. Andreyev et al. “ $\alpha$ -decay spectroscopy of the new isotope  $^{192}\text{At}$ ”. *Phys. Rev. C* 73 (2 Feb. 2006), p. 024317. DOI: [10.1103/PhysRevC.73.024317](https://doi.org/10.1103/PhysRevC.73.024317). URL: <https://link.aps.org/doi/10.1103/PhysRevC.73.024317>.
- [10] D. T. Doherty et al. “Solving the Puzzles of the Decay of the Heaviest Known Proton-Emitting Nucleus  $^{185}\text{Bi}$ ”. *Phys. Rev. Lett.* 127 (20 Nov. 2021), p. 202501. URL: <https://doi.org/10.1103/PhysRevLett.127.202501>.
- [11] K. S. Krane. “Introductory Nuclear Physics” (2008).
- [12] National Nuclear Data Center, Chart of Nuclides, Brookhaven National Laboratory, <https://www.nndc.bnl.gov/nudat3/>.
- [13] B. Blank and R. D. Page. “Charged-Particle Radioactive Decays”. In: *Handbook of Nuclear Physics*. Ed. by I. Tanihata, H. Toki, and T. Kajino. Singapore: Springer Nature Singapore, 2020, pp. 1–44. ISBN: 978-981-15-8818-1. URL: [https://doi.org/10.1007/978-981-15-8818-1\\_44-1](https://doi.org/10.1007/978-981-15-8818-1_44-1).
- [14] M. G. Mayer. “Nuclear Configurations in the Spin-Orbit Coupling Model. I. Empirical Evidence”. *Phys. Rev.* 78 (1 Apr. 1950), pp. 16–21. URL: <https://doi.org/10.1103/PhysRev.78.16>.
- [15] G. R. Choppin. *Radiochemistry and Nuclear Chemistry (Third Edition)*. Ed. by G. R. Choppin et al. Butterworth-Heinemann, 2002. URL: <https://doi.org/10.1016/B978-0-7506-7463-8.X5000-6>.
- [16] W. D. Loveland, D. J. Morrissey, and G. T. Seaborg. *Modern nuclear chemistry*. Ed. by W. D. Loveland. 2nd edition. Hoboken, NJ: John Wiley Sons, Inc, 2017, p. 744. ISBN: 978-1-119-32848-3.
- [17] J. O. Rasmussen. “Alpha-Decay Barrier Penetrabilities with an Exponential Nuclear Potential: Even-Even Nuclei”. *Phys. Rev.* 113 (6 Mar. 1959), pp. 1593–1598. URL: <https://doi.org/10.1103/PhysRev.113.1593>.
- [18] D. Karlgren et al. “Alpha Decay Hindrance Factors: A Probe of Mean Field Wave Functions”. *Phys. Rev. C* 73 (May 2004). URL: <https://doi.org/10.1103/PhysRevC.73.064304>.
- [19] C. Qi, R. Liotta, and R. Wyss. “Recent developments in radioactive charged-particle emissions and related phenomena”. *Progress in Particle and Nuclear Physics* 105 (2019), pp. 214–251. ISSN: 0146-6410. URL: <https://doi.org/10.1016/j.ppnp.2018.11.003>.

- [20] B. Blank et al. “Evaluation of fusion-evaporation cross-section calculations”. *Nucl. Instr. Methods Phys. Res., Sect. B: Beam Interactions with Materials and Atoms* 416 (2018), pp. 41–49. ISSN: 0168-583X. URL: <https://doi.org/10.1016/j.nimb.2017.12.003>.
- [21] M. Thoennessen. “Fusion-Evaporation Reactions”. In: *The Discovery of Isotopes: A Complete Compilation*. Cham: Springer International Publishing, 2016, pp. 197–226. ISBN: 978-3-319-31763-2. URL: [https://doi.org/10.1007/978-3-319-31763-2\\_11](https://doi.org/10.1007/978-3-319-31763-2_11).
- [22] K. H. Schmidt et al. “Some remarks on the error analysis in the case of poor statistics”. *Zeitschrift für Physik A Atoms and Nuclei* 316.1 (Feb. 1984), pp. 19–26. ISSN: 0939-7922. URL: <https://doi.org/10.1007/BF01415656>.
- [23] K. Schmidt. “A new test for random events of an exponential distribution”. *Eur. Phys. J. A* 8 (July 2000), pp. 141–145. URL: [10.1007/s100500070129](https://doi.org/10.1007/s100500070129).
- [24] J. Sarén et al. “Absolute transmission and separation properties of the gas-filled recoil separator RITU”. *Nucl. Instr. Methods Phys. Res., Sect. A* 654.1 (2011), pp. 508–521. ISSN: 0168-9002. URL: <https://doi.org/10.1016/j.nima.2011.06.068>.
- [25] M. Leino et al. “Gas-filled recoil separator for studies of heavy elements”. *Nucl. Instr. Methods Phys. Res., Sect. B* 99.1–4 (1995), pp. 653–656. ISSN: 0168-583X. URL: [https://doi.org/10.1016/0168-583X\(94\)00573-7](https://doi.org/10.1016/0168-583X(94)00573-7).
- [26] Y. T. Oganessian et al. “The average equilibrium charge-states of heavy ions with  $Z > 60$  stripped in He and H<sub>2</sub>”. *Z Phys D - Atoms, Molecules and Clusters* 21 (1 Mar. 1991). URL: <https://doi.org/10.1007/BF01426353>.
- [27] K. E. Gregorich et al. “Attempt to confirm superheavy element production in the  $^{48}\text{Ca} + ^{238}\text{U}$  reaction”. *Phys. Rev. C* 72 (1 July 2005), p. 014605. URL: <https://doi.org/10.1103/PhysRevC.72.014605>.
- [28] A. Ghiorso et al. “Sassy, a gas-filled magnetic separator for the study of fusion reaction products”. *Nucl. Instr. Methods Phys. Res., Sect. A* 269.1 (1988), pp. 192–201. ISSN: 0168-9002. URL: [https://doi.org/10.1016/0168-9002\(88\)90877-7](https://doi.org/10.1016/0168-9002(88)90877-7).

- [29] <https://www.jyu.fi/science/en/physics/research/infrastructures/accelerator-laboratory/nuclear-physics-facilities/recoil-separators/ritu-gas-filled-separator>.
- [30] R. Page et al. “The GREAT spectrometer”. *Nucl. Instrum. Methods Phys. Res., Sect. B* 204.0 (2003), pp. 634–637. ISSN: 0168-583X. URL: [https://doi.org/10.1016/S0168-583X\(02\)02143-2](https://doi.org/10.1016/S0168-583X(02)02143-2).
- [31] Y. Khazov, A. Rodionov, and G. Shulyak. “Nuclear Data Sheets for  $A = 146$ ”. *Nuclear Data Sheets* 136 (2016), pp. 163–452. ISSN: 0090-3752. URL: <https://doi.org/10.1016/j.nds.2016.08.002>.
- [32] N. Nica. “Nuclear Data Sheets for  $A=158$ ”. *Nuclear Data Sheets* 141 (2017), pp. 1–326. ISSN: 0090-3752. URL: <https://doi.org/10.1016/j.nds.2017.03.001>.
- [33] C. Reich. “Nuclear Data Sheets for  $A = 159$ ”. *Nuclear Data Sheets* 113.1 (2012), pp. 157–363. ISSN: 0090-3752. URL: <https://doi.org/10.1016/j.nds.2012.01.002>.
- [34] C. Reich. “Nuclear Data Sheets for  $A = 162$ ”. *Nuclear Data Sheets* 108.9 (2007), pp. 1807–2034. ISSN: 0090-3752. URL: <https://doi.org/10.1016/j.nds.2007.07.002>.
- [35] C. Reich and B. Singh. “Nuclear Data Sheets for  $A = 163$ ”. *Nuclear Data Sheets* 111.5 (2010), pp. 1211–1469. ISSN: 0090-3752. URL: <https://doi.org/10.1016/j.nds.2010.04.001>.
- [36] P. Rahkila. “Grain—A Java data analysis system for Total Data Readout”. *Nucl. Instrum. Methods Phys. Res., Sect. A* 595.3 (2008), pp. 637–642. ISSN: 0168-9002. DOI: <https://doi.org/10.1016/j.nima.2008.08.039>.
- [37] A. K. Jain, A. Ghosh, and B. Singh. “Nuclear Data Sheets for  $A = 165$ ”. *Nuclear Data Sheets* 107.5 (2006), pp. 1075–1346. ISSN: 0090-3752. URL: <https://doi.org/10.1016/j.nds.2006.05.002>.
- [38] C. M. Baglin. “Nuclear Data Sheets for  $A = 166$ ”. *Nuclear Data Sheets* 109.5 (2008), pp. 1103–1382. ISSN: 0090-3752. URL: <https://doi.org/10.1016/j.nds.2008.04.001>.

- [39] C. M. Baglin. “Nuclear Data Sheets for  $A = 179$ ”. *Nuclear Data Sheets* 110.2 (2009), pp. 265–506. ISSN: 0090-3752. URL: <https://doi.org/10.1016/j.nds.2009.01.001>.
- [40] C. M. Baglin. “Nuclear Data Sheets for  $A = 183$ ”. *Nuclear Data Sheets* 134 (2016), pp. 149–430. ISSN: 0090-3752. URL: <https://doi.org/10.1016/j.nds.2016.04.002>.
- [41] E. McCutchan. “Nuclear Data Sheets for  $A = 180$ ”. *Nuclear Data Sheets* 126 (2015), pp. 151–372. ISSN: 0090-3752. DOI: <https://doi.org/10.1016/j.nds.2015.05.002>. URL: <https://www.sciencedirect.com/science/article/pii/S0090375215000137>.
- [42] F. G. Kondev et al. “Interplay between octupole and quasiparticle excitations in  $^{178}\text{Hg}$  and  $^{180}\text{Hg}$ ”. *Phys. Rev. C* 62 (4 Sept. 2000), p. 044305. URL: <https://10.1103/PhysRevC.62.044305>.
- [43] K. Auranen and E. McCutchan. “Nuclear Data Sheets for  $A=212$ ”. *Nuclear Data Sheets* 168 (2020), pp. 117–267. ISSN: 0090-3752. URL: <https://doi.org/10.1016/j.nds.2020.09.002>.
- [44] M. Kortelainen et al. “Nuclear energy density optimization”. *Phys. Rev. C* 82 (2 Aug. 2010), p. 024313. URL: <https://doi.org/10.1103/PhysRevC.82.024313>.
- [45] M. Kortelainen et al. “Nuclear energy density optimization: Large deformations”. *Phys. Rev. C* 85 (2 Feb. 2012), p. 024304. URL: <https://doi.org/10.1103/PhysRevC.85.024304>.
- [46] J. Bartel et al. “Towards a better parametrisation of Skyrme-like effective forces: A critical study of the SkM force”. *Nuclear Physics A* 386.1 (1982), pp. 79–100. ISSN: 0375-9474. URL: [https://doi.org/10.1016/0375-9474\(82\)90403-1](https://doi.org/10.1016/0375-9474(82)90403-1).
- [47] J. Dobaczewski, H. Flocard, and J. Treiner. “Hartree-Fock-Bogolyubov description of nuclei near the neutron-drip line”. *Nuclear Physics A* 422.1 (1984), pp. 103–139. ISSN: 0375-9474. URL: [https://doi.org/10.1016/0375-9474\(84\)90433-0](https://doi.org/10.1016/0375-9474(84)90433-0).

- [48] E. Chabanat et al. “A Skyrme parametrization from subnuclear to neutron star densities Part II. Nuclei far from stabilities”. *Nuclear Physics A* 635.1 (1998), pp. 231–256. ISSN: 0375-9474. URL: [https://doi.org/10.1016/S0375-9474\(98\)00180-8](https://doi.org/10.1016/S0375-9474(98)00180-8).
- [49] P. Klüpfel et al. “Variations on a theme by Skyrme: A systematic study of adjustments of model parameters”. *Phys. Rev. C* 79 (3 Mar. 2009), p. 034310. URL: <https://doi.org/10.1103/PhysRevC.79.034310>.
- [50] Michigan State University, Mass Explorer interface, <http://massexplorer.frib.msu.edu/>.
- [51] “Nuclear properties for astrophysical and radioactive-ion-beam applications (II)”. *Atomic Data and Nuclear Data Tables* 125 (2019), pp. 1–192. ISSN: 0092-640X. URL: <https://doi.org/10.1016/j.adt.2018.03.003>.
- [52] S. Liran and N. Zeldes. “A semiempirical shell-model formula”. *Atomic Data and Nuclear Data Tables* 17.5 (1976), pp. 431–441. ISSN: 0092-640X. URL: [https://doi.org/10.1016/0092-640X\(76\)90033-4](https://doi.org/10.1016/0092-640X(76)90033-4).
- [53] B. Singh and J. C. Roediger. “Nuclear Data Sheets for A=182”. *Nuclear Data Sheets* 111.8 (2010), pp. 2081–2330. ISSN: 0090-3752. URL: <https://doi.org/10.1016/j.nds.2010.08.001>.
- [54] C. M. Baglin. “Nuclear Data Sheets for A = 184”. *Nuclear Data Sheets* 111.2 (2010), pp. 275–523. ISSN: 0090-3752. URL: <https://doi.org/10.1016/j.nds.2010.01.001>.
- [55] J. Batchelder, A. Hurst, and M. Basunia. “Nuclear Data Sheets for A=186”. *Nuclear Data Sheets* 183 (2022), pp. 1–346. ISSN: 0090-3752. URL: <https://doi.org/10.1016/j.nds.2022.06.001>.
- [56] F. Kondev, S. Juutinen, and D. Hartley. “Nuclear Data Sheets for A=188”. *Nuclear Data Sheets* 150 (2018), pp. 1–364. ISSN: 0090-3752. URL: <https://doi.org/10.1016/j.nds.2018.05.001>.
- [57] B. Singh and J. Chen. “Nuclear Data Sheets for A=190”. *Nuclear Data Sheets* 169 (2020), pp. 1–390. ISSN: 0090-3752. URL: <https://doi.org/10.1016/j.nds.2020.10.001>.

- [58] C. M. Baglin. “Nuclear Data Sheets for  $A = 192$ ”. *Nuclear Data Sheets* 113.8 (2012), pp. 1871–2111. ISSN: 0090-3752. URL: <https://doi.org/10.1016/j.nds.2012.08.001>.





## **A Properties of the new $\alpha$ -decaying isotope $^{190}\text{At}$**

A manuscript submitted for publication in Physical Review C. As of 28.04.2023 the manuscript has been reviewed by the Referee selected by the journal, and the Referee recommends that it should be published.

# Properties of the new $\alpha$ -decaying isotope $^{190}\text{At}$

H. Kokkonen,<sup>1,\*</sup> K. Auranen,<sup>1</sup> J. Uusitalo,<sup>1</sup> S. Eeckhaudt,<sup>1</sup> T. Grahn,<sup>1</sup> P.T. Greenlees,<sup>1</sup>  
P. Jones,<sup>1,†</sup> R. Julin,<sup>1</sup> S. Juutinen,<sup>1</sup> M. Leino,<sup>1</sup> A.-P. Leppänen,<sup>1,‡</sup> M. Nyman,<sup>1,§</sup> J.  
Pakarinen,<sup>1</sup> P. Rahkila,<sup>1</sup> J. Sarén,<sup>1</sup> C. Scholey,<sup>1,¶</sup> J. Sorri,<sup>1,\*\*</sup> and M. Venhart<sup>1,2</sup>

<sup>1</sup>*Accelerator Laboratory, Department of Physics, University of Jyväskylä, FI-40014 Jyväskylä, Finland*

<sup>2</sup>*Institute of Physics, Slovak Academy of Sciences, SK-84511 Bratislava, Slovakia*

(Dated: March 20, 2023)

The  $\alpha$  decay of a new isotope  $^{190}\text{At}$  has been studied via  $^{109}\text{Ag}(^{84}\text{Sr},3n)^{190}\text{At}$  fusion-evaporation reaction by employing a gas-filled recoil separator. An  $\alpha$ -particle energy of 7750(20) keV and a half-life of  $1.0_{-0.4}^{+1.4}$  ms were measured. The measured decay properties correspond to an unhindered  $\alpha$  decay, suggesting the same spin and parity of ( $10^-$ ) as those of the final state of the decay. The systematics of the nearby nuclei and the predictions of selected atomic mass models were compared with the measured decay properties.

## I. INTRODUCTION

Large-scale calculations, for example, the finite-range droplet model [1] and the Hartee-Fock-Bogoliubov (HFB) method based on the D1S Gogny effective nucleon-nucleon interaction [2, 3], predict multitude of nuclear shapes in the  $Z>82$ ,  $N\leq 126$  region. According to the models, in their ground state nuclei are nearly spherical near the closed neutron shell  $N = 126$ . Towards the proton dripline, the nuclei start to become slightly oblately deformed, and as approaching the neutron midshell  $N = 104$ , nuclei become strongly prolate deformed.

Experimental observations support the above discussed shape systematics. For example, odd-mass astatine isotopes have been widely studied via  $\gamma$ -ray spectroscopy, see, for example, Refs. [4–7] and references therein. The  $9/2^-$  ( $\pi h_{9/2}$ ) ground states of astatine isotopes are observed to have a spherical or weakly oblate shape down to  $^{197}\text{At}$ . Additionally, in these isotopes an isomeric state with a spin and parity of  $1/2^+$  ( $\pi s_{1/2}$ ) is observed [8, 9]. The At nuclei are observed to become more deformed as the mass number is further decreased and the structure of ground state is observed to change to  $1/2^+$  at  $^{195}\text{At}$  [10, 11]. These results are consistent with the measured changes in the mean-square charge radius, magnetic dipole, and spectroscopic quadrupole moments obtained with laser spectroscopy [12]. Moving towards the most exotic astatine nuclei, the production yields are too low for  $\gamma$ -ray spectroscopy, and half-lives become too short to permit studies with laser spectroscopy. How-

ever,  $\alpha$ -decay spectroscopy is an efficient technique to study these nuclei as only a few observations are enough to define the  $\alpha$ -particle energy  $E_\alpha$ , half-life  $T_{1/2}$ , mass-excess  $\Delta$  and one proton separation energy  $S_p$ . The last two require prior knowledge of the mass excesses of the daughter nuclei, which, however, are often available from other sources. With the quantities above one can discuss fundamental questions, such as, (*i*) the strength of shell closures, (*ii*) location of the proton dripline and (*iii*) predictive power of atomic mass models. The  $\alpha$ -particle preformation factor and the overlap of the initial and final state wave functions can be studied by calculating the reduced decay width  $\delta^2$  and the hindrance factor  $HF$ . For example, in Ref. [13] the most neutron-deficient astatine isotope known to date,  $^{191}\text{At}$ , was studied via  $\alpha$ -decay spectroscopy.

In the present article an observation of a new isotope of astatine,  $^{190}\text{At}$ , is reported and its  $\alpha$ -decay properties are presented. The present data are used to address the fundamental questions (*i*) – (*iii*) as applicable. Although the odd-odd nuclei are generally speaking challenging to study, odd-odd bismuth, astatine, and francium have been observed to have a common feature. These nuclei often have a high-spin state ( $10^-$ ), low-spin state ( $3^+$ ) and occasionally there is observed to be a ( $7^+$ ) state see, for example, Refs. [14–16]. The most neutron-deficient odd-odd astatine isotope before this study was  $^{192}\text{At}$  [17]. It was observed to have two  $\alpha$ -decaying states of which the longer-living ( $9^-, 10^-$ ) state was proposed to result from a  $[\pi 2f_{7/2} \otimes \nu 1i_{13/2}]$  configuration. However, in less exotic isotopes of bismuth and astatine this state is associated with a  $[\pi 1h_{9/2} \otimes \nu 1i_{13/2}]$  coupling.

## II. EXPERIMENTAL DETAILS

To generate  $^{190}\text{At}$  nuclei in the fusion-evaporation reaction  $^{109}\text{Ag}(^{84}\text{Sr},3n)^{190}\text{At}$ , a  $^{190}\text{At}$  target with a thickness of  $1 \text{ mg/cm}^2$  was irradiated with  $^{84}\text{Sr}$  ion beam.

Typical beam intensity was 12 pA. The ions were accelerated with the K-130 cyclotron at the Accelerator Laboratory of the University of Jyväskylä (JYFL),

\* henna.e.kokkonen@jyu.fi

† Present address: iThemba LABS, Somerset West 7129, South Africa

‡ Present address: Radiation and Nuclear Safety Authority - STUK, Lähteentie 2, 96400 Rovaniemi, Finland

§ Present address: University of Helsinki, PL55, 00014 University of Helsinki, Finland

¶ Present address: MTC Limited, Ansty Park, Coventry CV79JU, United Kingdom.

\*\* Present address: Radiation and Nuclear Safety Authority - STUK, Jokiniemenkuja 1, 01370 Vantaa, Finland

Table I. The beam energies  $E_{\text{beam}}$ , the thickness of the carbon degrader foil  $d_c$  in front of the target, energy in the center of the target  $E_{\text{c.o.t.}}$ , and the irradiation times  $t$  used in this study.

$E_{\text{beam}}$ (MeV)	$d_c$ ( $\mu\text{g}/\text{cm}^2$ )	$E_{\text{c.o.t.}}$ (MeV)	$t$ (h)
380	-	367	38
380	200	356	22
390	-	377	89
390	100	372	32

the used beam energies and other experimental conditions are listed on Table I. The gas-filled recoil separator RITU (Recoil Ion Transport Unit [18, 19]) was used to select the fusion-evaporation residues, now called recoils, and to transport them to the focal plane of RITU. At the GREAT (Gamma Recoil Electron Alpha Tagging [20]) spectrometer in the focal plane the recoils passed through a multiwire proportional counter (MWPC) and were subsequently implanted into a double-sided silicon strip detector (DSSD) with a thickness of 300  $\mu\text{m}$ . To increase the DSSD area, there were two DSSDs side by side, each with 40 vertical and 60 horizontal strips with strip width of 1 mm. The DSSD and MWPC were used to select recoils from scattered beam and from target-like particles with the time-of-flight between the detectors and the energy loss of the particles in the MWPC. An event in the DSSD that did not generate a MWPC signal was considered as a decay. The calibration of the DSSD energy response was performed using well-known  $\alpha$  activities produced in the  $^{78}\text{Kr} + ^{92}\text{Mo}$  reaction with an energy of  $E = 365$  MeV. The  $\alpha$ -decaying isotopes used in the calibration were  $^{150}\text{Dy}$ ,  $^{163}\text{W}$ ,  $^{162}\text{W}$ ,  $^{167}\text{Os}$ ,  $^{166}\text{Os}$ , and  $^{167\text{m}}\text{Ir}$ . Data for each detector channel were collected and timed with a 100 MHz clock. The data were analyzed with the GRAIN [21] software package to track decay chains containing two or three decay events.

### III. RESULTS AND DISCUSSION

The events associated with  $^{190}\text{At}$  were selected using spatial and temporal correlations. The recoil-implantation event had to be followed by at least two  $\alpha$ -decay events in the same pixel of the DSSD to be considered as a decay of the new isotope. Additionally, recoil implantation and the first  $\alpha$  decay must occur within 10 ms time window. The first and second  $\alpha$ -particle energies of such event chains are displayed in Fig.1. One should notice that the correlation matrix is effectively free of randomly correlated background events around the marked  $^{190}\text{At}$  decay chains.

The  $^{190}\text{At}$   $\alpha$ -decay chains observed in this study are displayed in Fig. 2. Three different events of  $\alpha$ -decay were observed with an average  $\alpha$ -particle energy of  $E_\alpha = 7750(20)$  keV and half-life  $T_{1/2} = 1.0_{-0.4}^{+1.4}$  ms. The half-

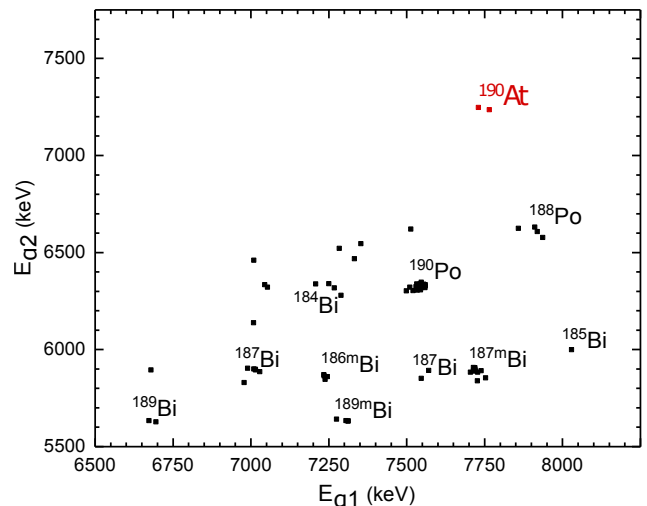


Figure 1. The energies of the first two  $\alpha$  particles observed in the same pixel of the DSSD as the preceding recoil implantation event. The first decay must occur within 10 ms from the recoil implantation events. The previously known nuclei [22] are indicated with black.

life was extracted with the Schmidt's maximum likelihood method [25], and the quoted  $\alpha$ -particle energy is the arithmetic mean of the  $\alpha$ -particle energies of the individual events. Additionally, the measured  $\alpha$ -particle energies are assumed to be free from  $\alpha$ -electron summing [26, 27] since significantly more statistics would be required to address this effect in detail. The analysis using Schmidt's radioactive decay probability test [28] was executed for the measured decay times. The decay times fit to the limits of the test and therefore the events are likely to originate from a decay of single radioactive species with a probability greater than 90%. Two of the events correlate with  $^{186}\text{Bi}$  7242 keV  $\alpha$  particles, and the full decay sequence is  $^{190}\text{At} \xrightarrow{\alpha} ^{186}\text{Bi} \xrightarrow{\alpha} ^{182}\text{Tl} \xrightarrow{\beta+/\text{EC}} ^{182}\text{Hg} \xrightarrow{\alpha} ^{178}\text{Pt}$ . The DSSD is insensitive to  $\beta+$  decay and electron capture, and therefore the  $^{182}\text{Tl} \rightarrow ^{182}\text{Hg}$  step remains unobserved.

From the measured  $\alpha$ -particle energy, a  $Q_\alpha$  value of 7920(20) keV was calculated by assuming a ground state to ground state  $\alpha$  decay. In Fig. 3 the deduced  $Q_\alpha$  value is compared to those of other neutron-deficient astatine isotopes. The present value fits well to the systematics and therefore the possible deviation arising from this assumption is likely of the order of some tens of kiloelectronvolts, if any. In Fig. 3 the  $Q_\alpha$  values predicted by selected mass models, Finite Range Droplet Model (FRDM [29]), shell model of Liran and Zeldes, and the average of six models based on different energy-density functionals EDF (SkP [30], SLy4 [31], SV-min [32], SkM\* [33], UNEDF0 [34], and UNEDF1 [35]) are also shown. The Mass Explorer interface [36] was used to obtain the EDF values. The measured  $Q_\alpha$  value of  $^{190}\text{At}$  is best reproduced by the FRDM when considering the three

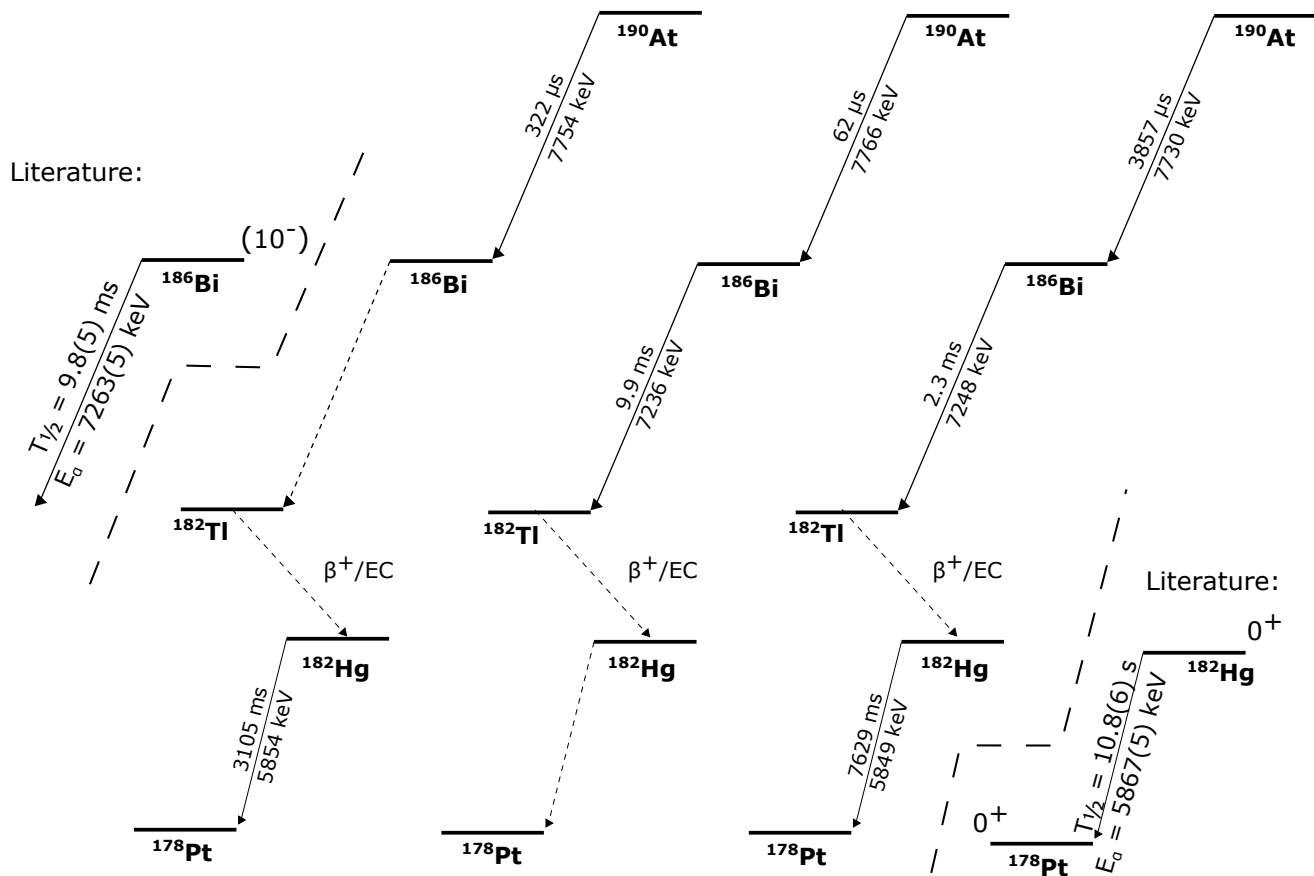


Figure 2. The recorded decay data of  $^{190}\text{At}$   $\alpha$ -decay chains observed in this study. The decays that were not observed are marked with a dashed line. The literature data are expressed above and below the thicker dashed lines [23, 24].

selected mass models. Also the EDF is close to the measured value. However, it should be noted that the EDF data are unavailable for the most exotic odd-odd nuclei as indicated by the dashed lines. The model of Liran and Zeldes diverges from the measured values of the most exotic isotopes being still accurate for  $N \geq 109$  within  $\pm 200$  keV. FRDM deviates from the measured values for  $N \sim 115$  isotopes significantly, but again reproduces the experimental values well closer ( $N \geq 118$ ) to the  $N=126$  shell closure.

The reduced decay width and the  $\alpha$ -decay hindrance factor deduced via the Rasmussen method [37] are  $\delta^2 = 70_{-50}^{+70}$  keV and  $HF = 1.0_{-0.5}^{+1.9}$ . The results were extracted using the half-life and the  $\alpha$ -particle energy of the present work, and by assuming a 100%  $\alpha$ -decay branch and an emission of s-wave  $\alpha$ -particles. The HF was deduced by normalizing  $\delta^2(^{190}\text{At})$  to that calculated from the  $\alpha$ -decay properties of  $^{212}\text{Po}$  [38]. As the theoretical prediction for the  $\beta$ -decay half-life is in the order of 600 ms [29], the  $\alpha$  decay is expected to dominate. The spin

and parity of the daughter nucleus  $^{186}\text{Bi}$  has been proposed to be  $(10^-)$  based on the systematics [39]. As the obtained  $\alpha$ -decay hindrance factor is close to unity, the initial and final states of the  $\alpha$ -decay are likely to have the same spin and parity. Therefore, we suggest that the presently observed  $\alpha$ -decay activity is from a  $(10^-)$  state in  $^{190}\text{At}$ . Additionally, fusion-evaporation reactions tend to favor high-spin states. This high spin is possible only to achieve if the wave functions of the  $\alpha$ -decaying state involve Nilsson orbitals arising from  $\nu i_{13/2}$ ,  $\pi h_{9/2}$ ,  $\pi f_{7/2}$  spherical parentage.

Proton-decay energy for  $^{190}\text{At}$  has been predicted [40] to be higher than 1 MeV, thus it is interesting to consider whether the presently observed state could proton decay. The mass excess of the new isotope 7200(30) keV was extracted by using the presently deduced  $Q_\alpha$  value, and mass excesses of the daughter nucleus and the  $\alpha$  particle, -3145(17) keV and 2424.91587(15) keV, respectively [41]. The proton-decay energy of  $^{190}\text{At}$  can be deduced as the mass-excesses of the decay products  $^{189}\text{Po}$  [-1422(22) keV

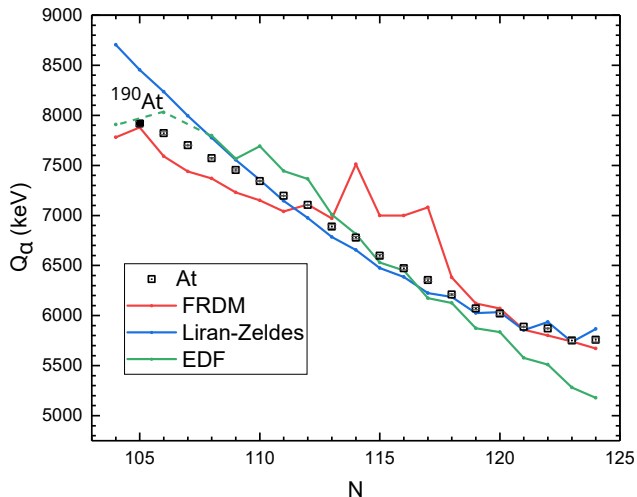


Figure 3. Ground state  $\alpha$ -decay energies  $Q_\alpha$  of astatine isotopes. The  $Q_\alpha$  of  $^{190}\text{At}$  (neutron number 105) extracted from the present study is indicated in the figure (solid symbol), as the rest of the experimental values marked with open symbols are from literature [41]. Solid lines express the predicted values from selected mass models from FDMR(2012) [29], Liran-Zeldes [42], and EDF (SkP [30], SLy4 [31], SV-min [32], SkM\* [33], UNEDF0 [34], and UNEDF1 [35]). The Mass Explorer interface [36] was used to obtain the EDF values. The EDF does not provide data for the most exotic odd-odd nuclei and therefore an interpolation is indicated with the dashed line.

[41]) and proton [7288.971064(13) keV [41]] are known. The extracted proton-decay Q value was 1330(40) keV. The partial half-life of a possible proton decay was approximated with a WKB integral by assuming that the proton is emitted from a  $h_{9/2}$  state. The resulting partial half-life for the proton decay was 30 s and therefore the proton decay cannot compete with the  $\alpha$  decay. This fits with the fact that, despite the careful analysis, the proton decay remained unobserved in this experiment. Similar conclusion can be made if the emitted proton is assumed to occupy an  $f_{7/2}$  orbital as the calculated half-life was 90 ms. If an emission from a  $\pi s_{1/2}$  orbital is considered,

the partial half-life is reduced to 2.5 ms, which is close to the measured half-life. However, it should be noted that it is not possible to obtain ( $10^-$ ) state by any expected coupling of the  $s_{1/2}$  proton. The above-mentioned proton emission half-lives assume spherical nucleus which might be far reaching, however, the quoted values can be taken as order of magnitude estimate and can be used to assess whether the proton decay can compete with the  $\alpha$  decay or not.

#### IV. SUMMARY

A new exotic neutron-deficient isotope of astatine,  $^{190}\text{At}$ , was produced and identified. The isotope was produced using a fusion-evaporation reaction and studied by means of its  $\alpha$ -decay properties. The identified  $\alpha$ -decay properties are an  $\alpha$ -particle energy and a half-life, 7750(20) keV and  $1.0^{+1.4}_{-0.4}$  ms, respectively. The  $\alpha$  decay was concluded to be unhindered and therefore, a spin and parity of ( $10^-$ ) was proposed for the decaying state of  $^{190}\text{At}$ . Using the determined decay properties, the possibility of proton emission was considered. It was found to be unable to compete with the  $\alpha$  decay. The measured  $\alpha$ -decay properties were compared with the systematics and also predictions of the selected atomic mass models.

#### V. ACKNOWLEDGMENTS

This work was supported by the Academy of Finland under the Contracts No. 323710, 347154, and 353786 (Personal research projects, KA). The contribution of M.V. was supported by the Slovak Research and Development Agency under contract No. APVV-20-0532, Slovak grant agency VEGA (contract No. 2/0067/21).

#### Data availability

The data obtained in the present work and the corresponding metadata are available from [link under preparation]

- [1] P. Möller, A. Sierk, R. Bengtsson, H. Sagawa, and T. Ichikawa, *Atomic Data and Nuclear Data Tables* **98**, 149 (2012).
- [2] S. Hilaire and M. Girod, *Eur. Phys. J. A* **33**, 237–241 (2007).
- [3] S. Hilaire and M. Girod, AMEDEC database, [https://www-phynu.cea.fr/science\\_en\\_ligne/carte\\_potentiels\\_microscopiques/carte\\_potentiel\\_nucleaire\\_eng.htm](https://www-phynu.cea.fr/science_en_ligne/carte_potentiels_microscopiques/carte_potentiel_nucleaire_eng.htm).
- [4] T. P. Sjoreen, D. B. Fossan, U. Garg, A. Neskakis, A. R. Poletti, and E. K. Warburton, *Phys. Rev. C* **25**, 889 (1982).
- [5] K. Andgren, U. Jakobsson, B. Cederwall, J. Uusitalo, T. Bäck, S. J. Freeman, P. T. Greenlees, B. Hadinia,

- A. Hugues, A. Johnson, P. M. Jones, D. T. Joss, S. Juutinen, R. Julin, S. Ketelhut, A. Khaplanov, M. Leino, M. Nyman, R. D. Page, P. Rahkila, M. Sandzelius, P. Sapple, J. Sarén, C. Scholey, J. Simpson, J. Sorri, J. Thomson, and R. Wyss, *Phys. Rev. C* **78**, 044328 (2008).
- [6] K. Auranen, J. Uusitalo, S. Juutinen, U. Jakobsson, T. Grahm, P. T. Greenlees, K. Hauschild, A. Herzán, R. Julin, J. Konki, M. Leino, J. Pakarinen, J. Partanen, P. Peura, P. Rahkila, P. Ruotsalainen, M. Sandzelius, J. Sarén, C. Scholey, J. Sorri, and S. Stolze, *Phys. Rev. C* **91**, 024324 (2015).
- [7] K. Auranen, J. Uusitalo, S. Juutinen, H. Badran, F. Defranchi Bisso, D. Cox, T. Grahm, P. T. Green-

- lees, A. Herzáñ, U. Jakobsson, R. Julin, J. Konki, M. Leino, A. Lightfoot, M. J. Mallaburn, O. Neuvonen, J. Pakarinen, P. Papadakis, J. Partanen, P. Rahkila, M. Sandzelius, J. Sarén, C. Scholey, J. Sorri, S. Stolze, and Y. K. Wang, *Phys. Rev. C* **97**, 024301 (2018).
- [8] K. Auranen, J. Uusitalo, S. Juutinen, U. Jakobsson, T. Grahm, P. T. Greenlees, K. Hauschild, A. Herzáñ, R. Julin, J. Konki, M. Leino, J. Pakarinen, J. Partanen, P. Peura, P. Rahkila, P. Ruotsalainen, M. Sandzelius, J. Sarén, C. Scholey, J. Sorri, and S. Stolze, *Phys. Rev. C* **90**, 024310 (2014).
- [9] K. Auranen, J. Uusitalo, S. Juutinen, H. Badran, F. D. Bisso, D. Cox, T. Grahm, P. T. Greenlees, A. Herzáñ, U. Jakobsson, R. Julin, J. Konki, M. Leino, A. Lightfoot, M. Mallaburn, O. Neuvonen, J. Pakarinen, P. Papadakis, J. Partanen, P. Rahkila, M. Sandzelius, J. Sarén, C. Scholey, J. Sorri, and S. Stolze, *Phys. Rev. C* **95**, 044311 (2017).
- [10] M. Nyman, S. Juutinen, I. Darby, S. Eeckhaudt, T. Grahm, P. T. Greenlees, U. Jakobsson, P. Jones, R. Julin, S. Ketelhut, H. Kettunen, M. Leino, P. Nieminen, P. Peura, P. Rahkila, J. Sarén, C. Scholey, J. Sorri, J. Uusitalo, and T. Enqvist, *Phys. Rev. C* **88**, 054320 (2013).
- [11] H. Kettunen, T. Enqvist, M. Leino, K. Eskola, P. Greenlees, K. Helariutta, P. Jones, R. Julin, S. Juutinen, H. Kankaanpää, H. Koivisto, P. Kuusiniemi, M. Muikku, P. Nieminen, P. Rahkila, and J. Uusitalo, *Eur Phys J A* **16**, 457–467 (2003).
- [12] J. G. Cubiss, A. E. Barzakh, M. D. Seliverstov, A. N. Andreyev, B. Andel, S. Antalic, P. Ascher, D. Atanasov, D. Beck, J. Bieroñ, K. Blaum, C. Borgmann, M. Breitenfeldt, L. Capponi, T. E. Cocolios, T. Day Goodacre, X. Derckx, H. De Witte, J. Elseviers, D. V. Fedorov, V. N. Fedosseev, S. Fritzsche, L. P. Gaffney, S. George, L. Ghys, F. P. Heßberger, M. Huyse, N. Imai, Z. Kalaninová, D. Kisler, U. Köster, M. Kowalska, S. Kreim, J. F. W. Lane, V. Liberati, D. Lunney, K. M. Lynch, V. Manea, B. A. Marsh, S. Mitsuoka, P. L. Molkanov, Y. Nagame, D. Neidherr, K. Nishio, S. Ota, D. Pauwels, L. Popescu, D. Radulov, E. Rapisarda, J. P. Revill, M. Rosenbusch, R. E. Rossel, S. Rothe, K. Sandhu, L. Schweikhard, S. Sels, V. L. Truesdale, C. Van Beveren, P. Van den Bergh, Y. Wakabayashi, P. Van Duppen, K. D. A. Wendt, F. Wienholtz, B. W. Whitmore, G. L. Wilson, R. N. Wolf, and K. Zuber, *Phys. Rev. C* **97**, 054327 (2018).
- [13] H. Kettunen, T. Enqvist, T. Grahm, P. Greenlees, P. Jones, R. Julin, S. Juutinen, A. Keenan, P. Kuusiniemi, M. Leino, A.-P. Leppänen, P. Nieminen, J. Pakarinen, P. Rahkila, and J. Uusitalo, *Eur. Phys. J. A* **17**, 537–558 (2003).
- [14] M. Huyse, P. Decrock, P. Dendooven, G. Reusen, P. Van Duppen, and J. Wauters, *Phys. Rev. C* **46**, 1209 (1992).
- [15] P. Van Duppen, P. Decrock, P. Dendooven, M. Huyse, G. Reusen, and J. Wauters, *Nuclear Physics A* **529**, 268 (1991).
- [16] J. Uusitalo, J. Sarén, S. Juutinen, M. Leino, S. Eeckhaudt, T. Grahm, P. T. Greenlees, U. Jakobsson, P. Jones, R. Julin, S. Ketelhut, A.-P. Leppänen, M. Nyman, J. Pakarinen, P. Rahkila, C. Scholey, A. Semchenkov, J. Sorri, A. Steer, and M. Venhart, *Phys. Rev. C* **87**, 064304 (2013).
- [17] A. N. Andreyev, S. Antalic, D. Ackermann, S. Franchoo, F. P. Heßberger, S. Hofmann, M. Huyse, I. Kojouharov, B. Kindler, P. Kuusiniemi, S. R. Leshner, B. Lommel, R. Mann, G. Münzenberg, K. Nishio, R. D. Page, J. J. Ressler, B. Streicher, S. Saro, B. Sulignano, P. V. Duppen, and D. R. Wiseman, *Phys. Rev. C* **73**, 024317 (2006).
- [18] J. Sarén, J. Uusitalo, M. Leino, and J. Sorri, *Nucl. Instr. Methods Phys. Res., Sect. A* **654**, 508 (2011).
- [19] M. Leino, J. Äystö, T. Enqvist, P. Heikkinen, A. Jokinen, M. Nurmi, A. Ostrowski, W. Trzaska, J. Uusitalo, K. Eskola, P. Armbruster, and V. Ninov, *Nucl. Instr. Methods Phys. Res., Sect. B* **99**, 653 (1995).
- [20] R. Page, A. Andreyev, D. Appelbe, P. Butler, S. Freeman, P. Greenlees, R.-D. Herzberg, D. Jenkins, G. Jones, P. Jones, D. Joss, R. Julin, H. Kettunen, M. Leino, P. Rahkila, P. Regan, J. Simpson, J. Uusitalo, S. Vincent, and R. Wadsworth, *Nucl. Instrum. Methods Phys. Res., Sect. B* **204**, 634 (2003).
- [21] P. Rahkila, *Nucl. Instrum. Methods Phys. Res., Sect. A* **595**, 637 (2008).
- [22] Brookhaven National Laboratory, National Nuclear Data Center, <https://www.nndc.bnl.gov/>.
- [23] B. Singh and J. C. Roediger, *Nuclear Data Sheets* **111**, 2081 (2010).
- [24] E. Achterberg, O. Capurro, and G. Marti, *Nuclear Data Sheets* **110**, 1673 (2009).
- [25] K. H. Schmidt, C. C. Sahn, K. Pielenz, and H. G. Clerc, *Zeitschrift für Physik A Atoms and Nuclei* **316**, 19 (1984).
- [26] F. Hessberger, S. Hofmann, G. Münzenberg, K.-H. Schmidt, P. Armbruster, and R. Hingmann, *Nuclear Instruments and Methods in Physics Research Section A: Accelerators, Spectrometers, Detectors and Associated Equipment* **274**, 522 (1989).
- [27] C. Theisen, A. Lopez-Martens, and C. Bonnelle, *Nuclear Instruments and Methods in Physics Research Section A: Accelerators, Spectrometers, Detectors and Associated Equipment* **589**, 230 (2008).
- [28] K. Schmidt, *Eur. Phys. J. A* **8**, 141–145 (2000).
- [29] P. Möller, M. Mumpower, T. Kawano, and W. Myers, *Atomic Data and Nuclear Data Tables* **125**, 1 (2019).
- [30] J. Dobaczewski, H. Flocard, and J. Treiner, *Nuclear Physics A* **422**, 103 (1984).
- [31] E. Chabanat, P. Bonche, P. Haensel, J. Meyer, and R. Schaeffer, *Nuclear Physics A* **635**, 231 (1998).
- [32] P. Klüpfel, P.-G. Reinhard, T. J. Bürvenich, and J. A. Maruhn, *Phys. Rev. C* **79**, 034310 (2009).
- [33] J. Bartel, P. Quentin, M. Brack, C. Guet, and H.-B. Håkansson, *Nuclear Physics A* **386**, 79 (1982).
- [34] M. Kortelainen, T. Lesinski, J. Moré, W. Nazarewicz, J. Sarich, N. Schunck, M. V. Stoitsov, and S. Wild, *Phys. Rev. C* **82**, 024313 (2010).
- [35] M. Kortelainen, J. McDonnell, W. Nazarewicz, P.-G. Reinhard, J. Sarich, N. Schunck, M. V. Stoitsov, and S. M. Wild, *Phys. Rev. C* **85**, 024304 (2012).
- [36] Michigan State University, Mass Explorer interface, <http://massexplorer.frib.msu.edu/>.
- [37] J. O. Rasmussen, *Phys. Rev.* **113**, 1593 (1959).
- [38] K. Auranen and E. McCutchan, *Nuclear Data Sheets* **168**, 117 (2020).
- [39] C. M. Baglin, *Nuclear Data Sheets* **99**, 1 (2003).

- [40] X. Yin, R. Shou, and Y. M. Zhao, *Phys. Rev. C* **105**, 064304 (2022).
- [41] M. Wang, W. Huang, F. Kondev, G. Audi, and S. Naimi, *Chinese Physics C* **45**, 030003 (2021).
- [42] S. Liran and N. Zeldes, *Atomic Data and Nuclear Data Tables* **17**, 431 (1976).